UNIVERSITY OF OKLAHOMA

GRADUATE COLLEGE

A SYSTEMATIC APPROACH TO DETERMINE THE OPTIMAL PRODUCTION RATE TO INHIBIT ASPHALTENE DEPOSITION

A THESIS

SUBMITTED TO THE GRADUATE FACULTY

in partial fulfillment of the requirements for the

Degree of

MASTER OF SCIENCE

By

ADESUWA NOSAKHARE
Norman, Oklahoma
2016

A SYSTEMATIC APPROACH TO DETERMINE THE OPTIMAL PRODUCTION RATE TO INHIBIT ASPHALTENE DEPOSITION

A THESIS APPROVED FOR THE
MEWBOURNE SCHOOL OF PETROLEUM AND GEOLOGICAL ENGINEERING

BY

_____
Dr. Rouzbeh G. Moghanloo, Chair

_____
Dr. Chandra Rai

_____
Dr. Xingru Wu

I dedicate this thesis to God Almighty. He alone gave me the opportunities, provision and perseverance needed to make it this far in my academic career. To Him be all the glory.

Acknowledgements

There's a popular saying that it takes a village to raise a child. In my case, I was blessed with a set of individuals handpicked by God to have unconditional love and faith in me, even when I found it hard to believe in myself. My academic journey has been graced by the presence of people without whom I would not be where I am today.

I would like to thank my advisor Dr. Moghanloo, for his unwavering support and guidance throughout my time at the University of Oklahoma and also my committee members, Dr. Rai, for his encouragement and financial support and Dr. Wu for walking me through a very crucial part of the journey. I would also like to thank the staff at MPGE, Summer Shije, Sonya Grant and Sheriee Parnell. Their encouragement and support through the years were priceless and did not go unnoticed.

To my friends who have become family, Fope Obadina. Ebony Tongo, LaTonya Simon, Tosin Oyeleke, Seyi Fadipe, Tobi Olorunsola, my BCF/ACF crew and fellow RCCG members, your encouragement, support and the good laughs shaped my experiences throughout this process. Thank you. To Omotola Adewuyi, Niyi Adewuyi and my Godson, Nathan Adewuyi, I strongly believe that God also had me in mind when he brought you to Norman. Your untiring faith in me kept me pressing on.

To my sisters, Eseosa, Ehi, Nosa and Osato, individually and collectively you have served as my backbone. Whenever I needed someone to lean on, complain to, laugh with and bounce ideas off of there was never a need to look too far. To my bethel

family and the Eluchies, who lovingly took the role of parents to me from the moment I entered the country to begin my undergraduate degree; I couldn't have done it without you.

Daddy and Mummy, where will I even begin. God will bless you for all that you've done and sacrificed to make me who I am today. Every day I pray for you, that as you have poured out your life to ensure that my siblings and I get the best of everything, the blessings of God that maketh rich and adds no sorrow will overflow in your lives.

Finally, I couldn't be done without mentioning the one the Lord kept for me, Taiwo Omotoso. You came into my life at the start of this degree program and I can't imagine what my experiences at OU would have been without you by my side. Words are really not enough but I love you and I'm grateful for you every day.

I'm thankful to God for blessing me with my very own village, the ones that have been there for me and been a part of my journey in more ways than I can reference. Although it's impossible to mention you all, thank you.

Table of Contents

List of Tables

List of Figures

Abstract

This thesis utilizes a systematic mathematical model, scaling analysis, to quantify the effect of production rate on asphaltene deposition, using a set of uniquely described mathematical equations modeled for the deposition process. Investigations to mitigate the effects of asphaltene deposition in both the well bore and porous media have recently focused on the first stage of formation; precipitation. Although the precipitation of asphaltene is necessary, it is not sufficient to guarantee its deposition; which poses the major problem for oil production. Quantification of these effects provides clarity on which individual factors create a significant impact on deposition. Results are compared to previously published, experimentally determined, significant factors for various asphaltene formation scenarios.

The study employs the 'order of one' scaling analysis method to identify the dimensionless groups that are specific to asphaltene deposition near the well bore and in production tubing. The describing equation includes the overall mass and momentum balance equations, precipitation and deposition equations and the reduction models for porosity and permeability. The dimensionless groups obtained are reduced to eradicate independence and the magnitudes of the individual variables are utilized to assess possible simplifying approximations. Assessment is based on the order of one scaling to determine the factors with greater magnitudes and identify their effects on the overall model. Governing equations, initial, boundary and auxiliary conditions are provided and described in detail to enable effective replication.

The minimum parametric representation of the describing equations are obtained and presented as twenty one dimensionless groups. These dimensionless groups

emphasize the importance of the concentration of asphaltene precipitate to the overall deposition rate. Results show that the deposition rate decreases significantly with a decrease in reservoir pressure, this is an important finding for secondary recovery. Optimum conditions, beyond which a significant increase in asphaltene deposition occurs, was determined at different production flow rates. Outcomes were correlated to experimental work done including the effect of CO_2 flooding on asphaltene deposition.

The main contribution of this work is to identify a set of dimensionless groups that aid retardation of the asphaltene deposition. The results obtained provide a template for the efficient design of experiments related to Asphaltene. In practice, the knowledge from this work will improve the effectiveness of flow assurance designs by ensuring that priority is placed on parameters with the most impact on asphaltene deposition in producing wells; saving time and costs associated with speculation.

Chapter 1: Introduction

In this chapter, we introduce asphaltenes, discuss the scope of the problem and main objectives of this work. We also introduce the structure of the different chapters in the following sections.

1.1 Scope of Problem

Asphaltenes are heavy hydrocarbon molecules that exist naturally in petroleum reservoir fluids. They are a solubility class that is usually defined as the fraction of crude oil that precipitates in aliphatic solvents, while remaining soluble in toluene (Speight, 1994). Asphaltene precipitation may occur during pressure depletion or during gas injection processes for Improved Oil Recovery (IOR). They consist of a variety of molecular species with molar masses of at least 1000 g/mol (Yaranton, 2000).

Asphaltene deposition is an important problem during oil production. This is because if ignored, it can result in formation damage and plugging of wellbore and surface facilities. This in turn leads to the accumulation of extra costs incurred by cleaning out and unplugging the wellbore. They can also lead to a significant reduction in permeability when formed in porous media, resulting in a decline in the rate of surface production.

In order to fully understand and find solutions to the problem that is asphaltene deposition, it is important to apprehend the process of formation of these deposits **Figure 1.1** shows the deposition process on the inner wall surface of a pipe. It is important to note that the asphaltene flocculates that deposit in the pipes can also be removed by erosion caused by fluid flow. The accumulation of deposited asphaltenes

minus what is being removed by erosion is what poses the deposition problems discussed in this work. A pictorial description is shown in the figure by Soulgani et al, (2010).

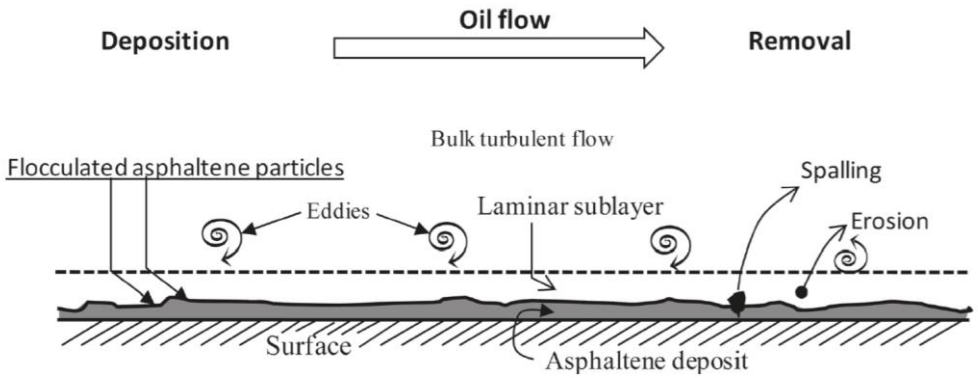

Figure 1.1 Schematic of the asphaltene deposition process, (Soulgani et al, 2010)

Asphaltenes are known to self-associate and or precipitate with changes in temperature, pressure or composition of the surrounding fluid. These precipitates are small particles in the order of a few microns estimated by visual observation. After precipitation, the small particles begin to agglomerate to form macro particles. The agglomeration process and size of the agglomerates also depend on the temperature and pressure of the solvent. These agglomerates easily adsorb on hydrophilic surfaces and also adhere to equipment surfaces forming deposits that could pose problems (Yaranton, 2000).

1.2 Research Objectives

In this work, emphasis is placed on the deposition of the aggregates, as the process of precipitation has been extensively studied in the past. The deposition process is scrutinized and mathematically defined using a set of pre-determined equations

describing the process. With the use a systemic mathematical approach called Scaling Analysis, important dimensionless groups are obtained that fully describe the asphaltene deposition process.

The aim of this work is to investigate conditions, with the help of the dimensionless groups, within which asphaltene deposition can be mitigated or delayed during production. Results obtained and discussed would be utilizable in the production industry to prevent the costs associated with the removal of asphalt deposition in the wells and in porous media. Also, information provided would help improve workplace safety, as engineers would be made aware of conditions within which asphaltene deposition can be expected, with additional information on how these conditions can be mitigated.

1.3 Chapter Overview

In Chapter 2, we review the background of asphaltene in oil production as it relates to precipitation and deposition. The chemistry behind the precipitation and conditions that encourage precipitation are outlined. The differences associated with deposition in pipes, that is the wellbore and in porous media are also outlined. In Chapter 3, the mathematical models usually used to describe deposition in both pipes and porous media are briefly introduced. The models chosen for this work are also discussed and shown along with some other models that were considered and are closely related to the deposition process modelled. Scaling Analysis is introduced as well and explained in ways that would enable the reader reproduce the work done, while creating opportunities for the procedure to be further utilized for other purposes.

In Chapter 4, the results obtained from this scaling analysis are presented for deposition in porous media and also in the pipes. These results are discussed and analyzed Emphasis is placed on deposition in pipes. Chapter 5 offers validation on the results obtained and trends proposed from experimental data. This validation is based on findings from of experimental data previously published. Finally, a conclusion is presented as a short summary of the work done throughout this thesis, and an idea of paths that could be taken in the future to improve on the findings of this research is also given under future work. Nomenclature, References and Appendix follow after conclusions and future works have been stated.

Chapter 2: Background and Literature Review

An in depth description of asphaltene deposition is provided in this chapter to give a well-rounded background and literature review of the problem. The different stages of the deposition process are discussed extensively and the major differences associated with deposition in porous media and in pipes are highlighted.

2.1 Asphaltene Precipitation

Asphaltene deposition can result from the production of heavy oils and crude reserves. These deposits reduce reservoir productivity, cause formation damage and expensive deterioration to production equipment (Yarranton, 2000). There have been several means investigated to possibly control and reduce its effect in both the well bore and reservoir. These investigations have recently focused on precipitation which is the first stage of formation. Dating back to 1982, different models have been created to develop an understanding of the existence of asphaltene.

The two major physical theories used to develop these models are that asphaltene is dissolved in crude oil completely; the real-solution theory , and that asphaltene exists in a colloidal suspension in crude oil; colloidal theory (Wang 2000). Both theories however agree that the ability to predict the thermodynamic properties of these crude oil systems is necessary to understand asphaltene precipitation. To achieve this, several thermodynamic models exist including cubic equations of state like the Redlich-Kwong and Peng Robinson equation.

These equations are sufficient for phase equilibrium and density calculations but tend to provide extremely low densities for liquids. Since asphaltene precipitation

occurs at reservoir conditions, in order to correctly model this process it is important that volumetric behavior at high pressure is captured accurately (Perdesen et al, 2007). It is also important that the model used can deal with asymmetric mixtures with molecules of varying sizes.

PC-SAFT is a thermodynamic model based on the Perturbed Chain version of the Statistical Associated Fluid Theory. It was developed for polymer systems and has shown promising results in modelling phase equilibrium of systems with heavy hydrocarbons like asphaltene (Panuganti et al, 2013). Some studies have concluded that gas injection increases the rate of asphaltene precipitation as it alters the solvent composition (Gonzalez, 2012). Other investigations on asphaltene precipitation as it relates to deposition have concluded that although asphaltene precipitation cannot be entirely prevented, the basic properties of the fluids can be controlled to ensure that precipitation is minimal.

Another method used to investigate the mechanism of asphaltene precipitation is with the use of a high-pressure flow experiment. In this experiment, a fluid sample is kept in a vessel at a pressure and temperature close to the reservoir conditions. The pressure is then dropped gradually until asphaltene precipitation is observed (Thawer et al., 1990). This result is checked against the typical APE phase diagram, where the upper asphaltene precipitation curve is usually above the bubble point pressure curve shown in **Figure**. **2.1**. As soon as the pressure goes into the APE curve, the asphaltenes in the crude precipitates out until the pressure reaches below the saturation pressure (Leontaritis, 2007). **Figure 2.2** shows a schematic of the Asphaltene precipitation curve envelope with pressure against temperature as in Figure 1 and also against composition.

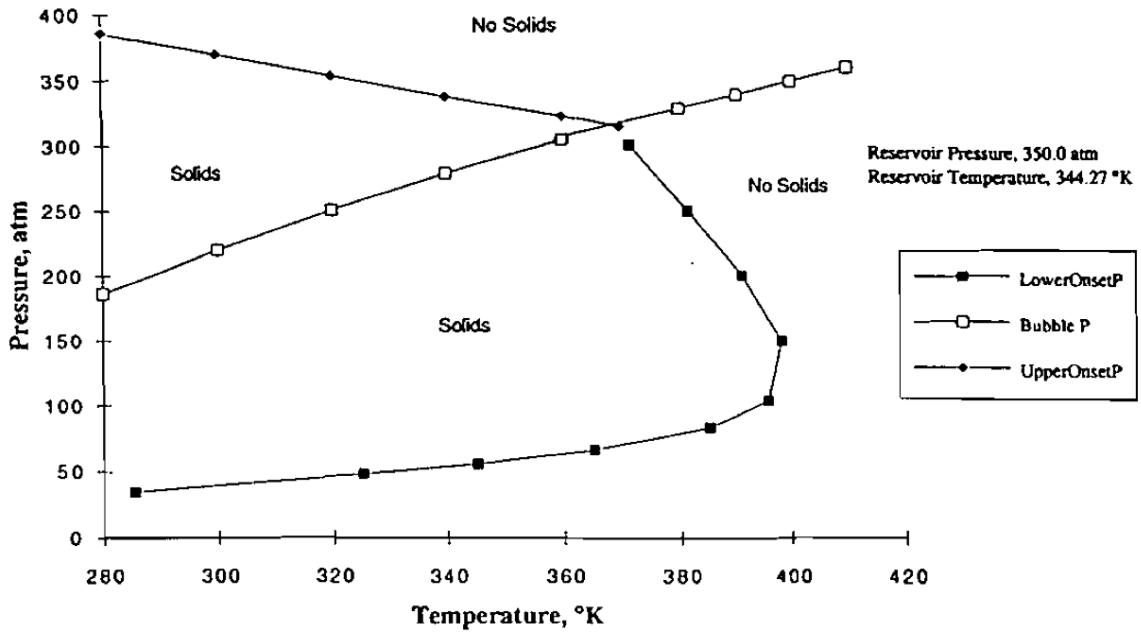

Figure. 2.1 Phase diagram of asphaltene precipitation envelope and bubble point pressure curve (Leontaritis, 2007)

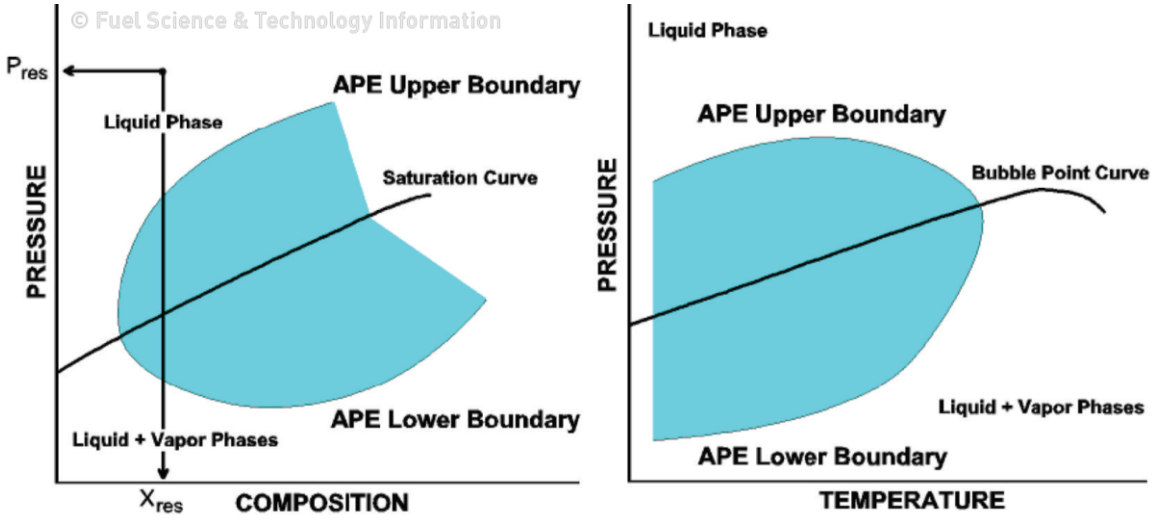

Figure. 2.2 Schematic of the asphaltene precipitation envelope against composition and temperature respectively (coined from Leontaritis, 2007)

The schematic shown in Figure 2 suggests that the changes in the pressure composition and the temperature affect equilibrium and could cause the precipitation and eventual deposition of asphaltene. The Envelope bounds the regions where precipitation occur for both the pressure against composition as well as against temperature. Where onset conditions occur at the envelope boundary. Within the APE, the amount of precipitated asphaltene increases with a decrease in pressure from the upper onset pressure to the oil saturation pressure. At the saturation pressure, the maximum value of precipitation is reached. Below the saturation pressure, precipitation decreases with a decrease in pressure (Leontaritis, 2007).

2.2 Asphaltene Aggregation

Asphaltenes aggregate where precipitation occur. This can be seen even in very dilute solutions of good solvents such as toluene. At the nanoscale, asphaltene aggregation begins to occur a precipitation concentration well below 100mg/L (Mullins, 2009). The point at which aggregation at the nanoscale begins to form has been studied by various researchers and is popularly referred to as the critical nanoaggregate concentration point (CNAC) (Painter et al, 2015). At higher precipitation concentrations however, the nanoaggregrates cluster about themselves to form micelles. The concentration at which the micellar formation begins is also known as the critical micelle concentration. These micelles continue to grow in size as collection of nanoaggregates continue. These different stages of aggregation mentioned were visually depicted in the work by Mullins, 2009 and is shown in **Figure 2.3**.

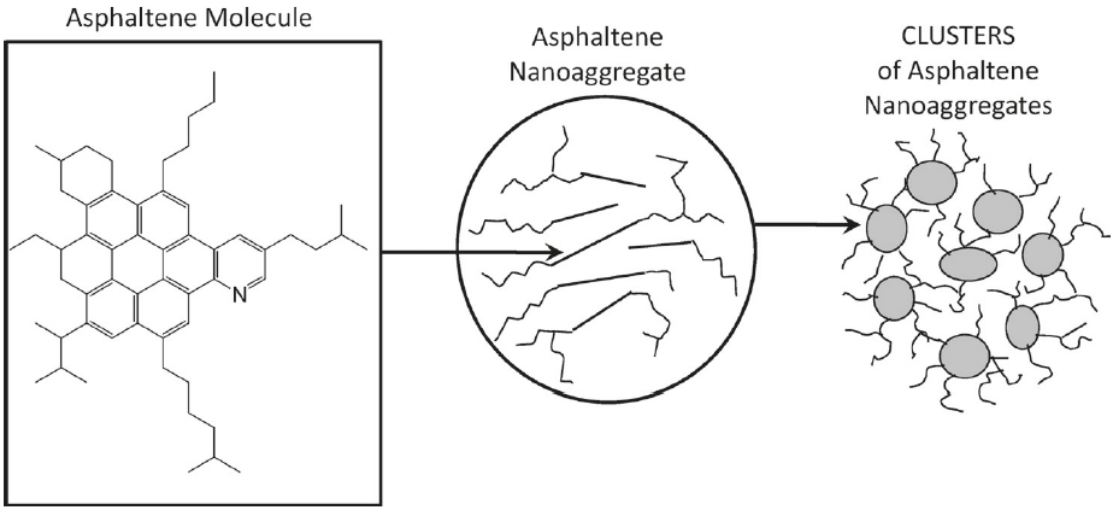

Figure. **2.3 Schematic of the asphaltene molecular architecture (left), formation of asphaltene nanoaggregates (center) and formation of micelle clusters by the nanoaggregrates (right) (Mullins, 2009)**

In general, asphaltene aggregates have been studied in sections based on the size of the aggregates been considered. However for the purpose of this work, aggregation would be discussed as a process regardless of the size; as all sizes of asphaltene aggregates can potentially deposit and cause problems in the wellbore and in porous media. Aggregation of the asphaltene particles is important for deposition to occur and larger aggregates would generally cause more plugging problems than smaller aggregates. This is because smaller aggregates in general stand a better chance of being entrained in the fluid flow during production. Reducing the amount of asphaltenes being deposited in place.

2.3 Asphaltene Deposition

Deposition of asphaltene, which is the third stage of solid asphaltene formation process, is a widespread problem because it affects processes in different industrial sectors depending on the location of its occurrence. In the reservoir it can lead to formation damage and in-situ plugging, also sub-surface and surface equipment plugging may occur during production. It remains an issue during refining and transportation where equipment and pipeline blockage, catalyst deactivation and capacity loss occur (Leontaritis, 1989). Asphaltene deposition near the wellbore and in the wellbore have a direct impact on the rate and costs associated with oil production. As a result, impact in these locations are further discussed in later sub sections.

The deposition rate of asphaltene much like precipitation and aggregation is strongly controlled by the concentration of precipitant. It has also been suggested that there may not be a critical precipitant concentration for asphaltene stability and deposition, and as such, it is necessary to investigate whether asphaltenes deposition can be seen at increasingly dilute precipitant concentrations (Hoepfner et al, 2013). As stated in the previous section, the detection mechanism, pressure drop, does not depend on the size of asphaltene aggregates, and sub micrometer asphaltenes can deposit to contribute to the instability detection. Although larger aggregate sizes have better chances of being deposited.

Several tests have been conducted to measure the rate of deposition as measured in a capillary. Wang and Buckley developed a displacement test technique to determine the deposit profile inside a capillary by monitoring the mass that exits the capillary as a function of time when a viscous fluid is forced through it; depicting the production

process (Wang and Buckley, 2006). There has also been experiments done to prove that there are certain critical conditions like shear rate below which asphaltene deposition will not occur.

According to Nabzar and Aguilera, when the shear rates are relatively low, asphaltene deposition follows the colloidal deposition scaling of diffusion limited deposition. An increase in the shear rate causes the asphaltenes to pass through a shear limited deposition process, and at high enough shear rates, no detectable deposition occurs. (Nabzar and Aguilera, 2008) This finding highlights the importance of hydrodynamics in asphaltene deposition.

There have been more interesting investigations done to determine regions of asphaltene deposition. Some including a critical aggregate size below which no deposition occur, effects of precipitant type and concentration and even location of deposits on deposition rate. It has also being insinuated tha deposition begins to occur before the precipitation of asphaltene can be detected by the use of standard techniques (Hoepfner et al, 2013). All the different investigations have been in a quest to determine the driving force of asphaltene deposition as a process.

In summary, asphaltenes are known to exist as particle colloids stabilized in suspension by resin molecules in solution (Joshi et al, 2001). Pressure depletion below the upper onset pressure and gas injections generally destabilizes the colloidal suspension of asphaltenes and resins, causing the asphaltenes to precipitate out of the crude oil. Further reduction in the reservoir pressure leads to an increase in the asphaltene precipitation which increases its concentration and aggregation into larger particles. These precipitates either flow as suspended particles or deposit onto the rock

surface near the wellbore. Deposition onto the rock surface could alter wettability, reduce the available pore space for fluids and reduce the permeability of the formation (Kohse et al, 2004). Deposition can also occur on the inner walls of the wellbore when flocculated asphaltene comes in contact with the walls or other deposited asphalts.

2.3.1 Asphaltene deposition in porous media

Asphaltene deposition in porous media is an issue because it creates blockages in the pore throat of the porous continuum in the subsurface. Thus hindering the flow of hydrocarbons to the surface for production. **Figure 2.4** shows a schematic of the asphaltene deposition problem in porous media (Civan, 2005). There are different models being utilized to describe the deposition process and effects in porous media but for our purposes, a modification of the Civan's model is utilized. This model divides the deposition process into three basic processes and they are also represented in figure 2.4. They are Surface deposition, Deposit Entrainment and Pore throat plugging. Together these processes combine to give the overall asphaltene deposition effect in porous media.

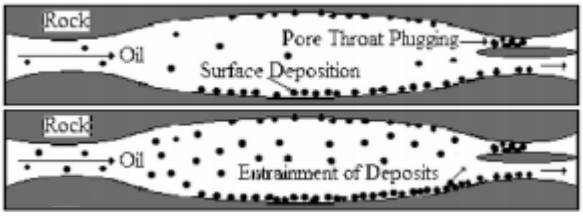

Figure 2.4 Schematic of Asphaltene deposition in porous media showing pore surface deposition, entrainment of deposits and pore throat plugging (Civan, 2005).

Surface deposition is the most dominant of the three processes describing deposition. It is the spontaneous attachment of particles to pore surfaces in the porous medium. It could possibly be triggered by favorable hydrodynamic conditions or even interactions between the asphaltene particles and the surface of the pore space, as shown in the diagram. Entrainment of the deposits and pore throat plugging are less dominant processes than the surface deposition and are not always realized.

Entrainment of the deposit is the continual transportation of the asphaltene particles in the fluid. This particles could either be produced with the crude oil or ultimately deposited along the porous medium at a farther location and time. As a result, continual particle entrainment is needed to prevent asphaltene deposition so that the particles are produced with the crude oil as opposed to hindering the production of the crude by plugging depositing in the pore space and eventually plugging pore throats.

According to the oilfield glossary, pore throats are small pore spaces at the point here two grains meet which connect two larger pore volumes. They are very important during oil production because the presence of a single pore throat can potentially double the amount of oil in place to be produced. If these pore throats are clogged, one might need to drill another well in order to access oil reservoirs that could have been accessed by existing wells. Entrained asphaltene particles could potentially block pore throats as shown in the Figure 2.4 and these can be attributed to being a resultant of asphaltene deposition in porous media.

2.3.2 Asphaltene deposition in pipes

Asphaltene deposition in pipes and in wellbores is also a serious issue encountered in oil production, not only does it pose economic problems like deposition in porous media specifically where pore throat plugging is an issue, It also poses safety concerns for both the workers and surrounding equipment. The associated problems are dependent on the location and extent of the asphaltene deposit in the pipes or wellbore.

Common resulting problems that are independent of the deposit location include increase in pressure levels in the pipes that could potentially lead to blow outs. These cause loss of equipment that is the pipes and other surrounding structures and also in extreme cases may cause injury and possibly death to employees in the vicinity. If the deposition occurs closer to the surface of the wellbore the risks become higher for employees also, surface facilities such as the pumps, valves, tubes, tanks and so on could be potentially damaged (Ramirez-Jaramillo et al, 2005).

Figure 2.5 shows a schematic of asphaltene deposition in a pipe (Mirzayi et al, 2013). As explained, it is very undesirable as it creates a significant decrease in production rate and also, remediation of a plugged wellbore is expensive and time consuming (Leontaritis, 1989). Some of the remediation techniques utilized include the use of asphaltene inhibiting chemicals or drilling the asphaltene plug.

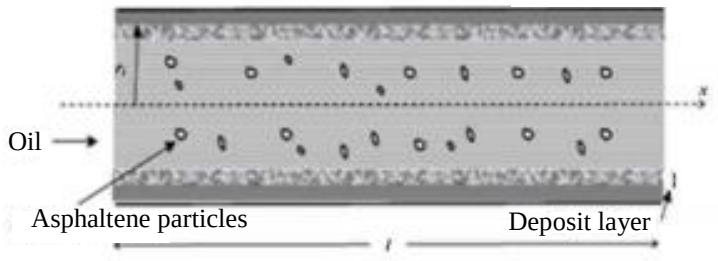

Figure 2.5. Schematic of Asphaltene deposition in pipes (Mirzayi et al, 2013).

Like with deposition in porous media, there are different models put together to describe the deposition process for both laminar and turbulent flows. These models would be described in Chapter 3. However the model utilized emphasizes the importance of the probability theorem and the probability that the asphaltene particles would stick to the pipe surface and also to the other particles already stuck on the pipe. Like shown in the figure a deposit layer is formed during deposition and this alters the diameter of the pipe, impeding flow and increasing pressure build up in the pipe.

In this work, existing mathematical models describing asphaltene deposition are utilized in a systematic scaling analysis method to assess the relative importance of the contributing factors affecting asphaltene deposition in both the wellbore and near wellbore regions. The models and results obtained from the analysis are further discussed in following chapters

Chapter 3: Mathematical models and Methods

In this chapter, three major sections are covered. They are the models utilizable for the comprehensive description of asphaltene deposition in porous media, models for the description of deposition in pipes and an introduction to the scaling analysis methodology used to analyze the models chosen for the deposition in both cases. The sections would be reviewed in the order described.

3.1 Asphaltene deposition models in porous media

Most of the models derived for the simulation of asphaltene deposition in porous media have been based solely on experimental data obtained either from laboratory core tests or from field simulations. Although, the results from field simulations can be said to better depict the actual deposition scenarios, Core testing has provided a means to isolate and study the different factors that sum up to create asphaltene deposition problems in the porous media near the wellbore.

3.1.1 Laboratory Core test simulation of asphaltene deposition

There are three major models that stemmed from laboratory core test analysis and they are discussed in order of publication time. In 1995, Civan modified a previously introduced parallel pathway model that was used to simulate the deposition of fine particles. The model classified all pore throats as either a plugging pathway or non-plugging pathway depending on the fluid flow through them (Wang, 2000). He included a source term for precipitation and porosity and permeability variability for the

deposition of paraffin and asphaltene. An energy balance was also introduced (Civan, 1995).

In developing a model, Ali and Islam considered the adsorption and mechanical entrapment of asphaltene. It was assumed that asphaltene existed in crude oil as particles and was readily deposited or adsorbed (Wang, 2000). This model was also a modification of the Civan's model as information from that model was utilized to simulate the mechanical entrapment. It was published in 1997. Other assumptions made were that the porous media was oil wet and a monolayer adsorption process was occurring (Ali and Islam, 1998). Finally in 1999, Wang further modified the model to simulate deposition of asphaltene and paraffin simultaneously and results obtained matched experimental data where ideal solution was used to simulate precipitation (Wang et al, 1999).

3.1.2 Field simulation of asphaltene deposition

The first model that simulated asphaltene deposition around a well with constant production rate and pseudo steady state flow was created by Leonaritis in 1998. It was assumed that asphaltene deposition occur only in near wellbore region and the area of formation damage caused by asphaltene deposition was constant (Wang, 2000). A simulation of asphaltene deposition in the near wellbore region within a radius of 5 feet and a production time of 5 hours was performed. The computational results of this model was unstable after three hours during experimentation (Leonaritis, 1998). A simple rule of thumb method was also used to determine the amount of particles that would be entrained in the fluid flow through the pores.

In the model by Ngheim et al. (1998) a liquid solid equilibrium precipitation process was adopted for asphaltene. Deposition was also simulated during primary recovery and CO2 flooding. And deposition was assumed to be driven solely by adsorption only. This assumption reduced the accuracy of results obtained from the model as several factors were observed that caused deposition in porous media besides adsorption (Leonaritis, 1998). In 2000 Wang and Civan created a model which is utilized in this work for the deposition of asphaltene in porous media. The model introduced the concepts of surface deposition, entrainment of particles and pore throat plugging as components that make up the deposition process. Reduction models were also incorporated for permeability and porosity to account for the changes encountered as deposition occurs. It was also the first model that could be used to simulate production from horizontal wells (Civan and Wang, 2005).

3.1.3 Applied model for deposition in porous media

The mathematical processes being considered were asphaltene deposition in the subsurface near the wellbore in the pipes. As previously mentioned, near the wellbore the deposition model by Civan and Wang (2000) was applied. The model is a modification of the Civan's model (1995) and is generally used for the deposition of paraffin and asphaltene. Some of the assumptions made in this model are listed below.

1. One dimensional horizontal flow
2. Negligible capillary pressure

The mass balance, momentum balance, precipitation model deposition model porosity and permeability reduction equations were combined to describe the overall deposition

process (Wang. 2000, pp 53-59). **Equation 3.1** represents the deposition equation utilized in this model. The first term on the right hand side represents the rate of asphaltene surface deposition with $\propto$ as its coefficient, the next represents the entrainment of asphaltene deposits in the bulk fluid and the last tern is the pore throat plugging rate, both having $\beta \; and \; \gamma$ coeeficients respectively. The other equations that make up this model are represented in **Appendix A**.

$$\frac{\partial E_A}{\partial t} = \propto C_A \phi - \beta E_A \left(v_L - v_{cr,L}\right) + \gamma u_L \, C_A \tag{3.1}$$

3.2 Asphaltene deposition models in pipes

Asphaltene deposition continues to be an issue for remediation even after the crude is past the porous media. In the wellbore asphaltene particles continue to aggregate and deposit over time on the surface of the inner pipe walls. Since the flow regimes and conditions in the wellbore and pipes differ significantly from that in porous media, it is necessary to for the deposition process in these regions to be modelled differently after particle fouling in chemical processes. Section 3.2.1 summarizes and classifies the different models that have been utilized to describe asphaltene deposition in the pipes.

3.2.1 Categories of Asphaltene deposition Models in pipes

There are different models that have been setup to define the process of asphaltene deposition in pipes and they have been widely grouped into two categories based on the approaches taken to reach the solution. They are the classical concept of turbulent flow and eddy diffusion and the stochastic approach (Shirdel, 2013)

Lin et al (1953) was amongst the first published authors to utilize the classical approach in modelling deposition in pipes. The idea was based off of the concept of mass transfer between a fluid stream that is turbulent and the surrounding walls. The concentration profile was calculated in the wall layer and a comparison of the model to experimental work was performed. Results showed a degree of agreement that proved that a correlation existed. Other researchers tried to create modifications to the model to get better agreement using the same concepts and similar approaches.

The stochastic approach is also popularly utilized by different researchers some include Cleaver and Yates (1975), Eskin et al, (2011) and Hutchinson et al (1971). In this approach a probabilistic theory is utilized to create the deposition model. Eskin et al, (2011) went ahead to perform experiments to verify the model using coquette devices and a fairly good agreement was realized. The stochastic approach has also been utilized to determine the mechanism of particle transport from fluid to the pipe surface as well as the size distribution of the asphaltene particles (Shirdel, 2013). Generally wax deposition models also follow the stochastic approach used to create models for asphaltene deposition in the wellbores and particulate fouling.

3.2.2 Applied model for deposition in pipes

Cleaver and Yates (1975) deposition model was used to derive the equation for asphaltene deposition in a pipe or wellbore in this work. The model uses the probability theorem as earlier stated and agrees with experimental data for particle deposition (Cleaver et al, 1975). They assumed that the particles are moved initially by turbulent diffusion and then entrained in the laminar sub layer as they get closer to the wall for

deposition. Asphaltene particles are also exhibited as solid spheres in this model (Shirdel, 2013).

Other equations applied to describe the overall process of deposition in pipes include rate of attachment and detachment of the particles. Mass and momentum conservation equations as well (Shirdel. 2013, pp. 186-188). The deposition equation used in this model is presented as **Equation 3.2**. All other equations used to describe the overall deposition for both processes are listed and described appropriately in **Appendix A**.

$$m_{da} = \frac{\partial}{\partial x} SP \left(\frac{0.084 \Delta C V_{avg} \sqrt{f/2}}{Sc^{2/3}} \right) \tag{3.2}$$

From the equation, m_{da} is the rate of solid asphaltene deposition, SP is a constant known as the sticking probability obtained from the probability theorem applied and Sc is the dimensionless Schmidt number, which is a ratio of the momentum diffusivity and mass diffusivity in the characterization of fluid flow.

The sticking probability is the probability that the molecules are trapped on the surface of the pipe and is attached to it. It can be deduced by a simple equation that includes the coverage area, which in this case is the inner walls of the pipe and the original probability that the material would stick. The sticking probability can also be assumed based of experimentally observations for example, if a material sticks to the walls of a pipe 4 out of 10 times its in contact then the sticking probability of the material to the pipe is 0.4. There are more complex ways to account for how materials stick but for our purposes, based on the equation utilized, the sticking probability seemed sufficient.

The procedure used to analyze the models described in this chapter is presented in the following section. Results obtained from the scaling analysis procedure was used to analyze the deposition equations for different conditions that may occur. Simplified versions of the equations are obtained and they highlight the factors that are major contributors to asphaltene deposition at different phases of production. Assumptions made for these mathematical models utilized for both deposition in porous media and in pipes and are listed below.

1. Flow is 1-Dimensional 2 phase flow
2. Isothermal flow conditions
3. Precipitation and aggregation already occurred, only the deposition process is considered

3.3 Scaling Analysis

The systematic methodology used to quantify the different factors affecting asphaltene deposition in the pipes and subsurface is called Scaling Analysis. According to William B. Krantz, scaling analysis is used to create dimensionless groups for sets of equations describing various processes. Most of the processes are chemical engineering reaction processes but they can also be used to describe other processes as long as the major describing equations are known.

This methodology, much like Buckingham pi creates dimensionless relations commonly referred to as pi groups. One advantage it has over the Buckingham pi method however, is that the scaling analysis results in the minimum parametric representation of the describing equations, which makes it possible to quantify the

different parameters and rank them in order of relevance to the entire process described. This is not the case with the Buckingham pi method, which only shows a non-quantifiable relationship like in the case of the Reynolds number (Krantz. 2007, xi-xiii).

The mathematical foundation of Scaling Analysis is in the Lie Group. This theory represent the best-developed theory of continuous symmetry of mathematical objects and structures. As a result, it is an indispensable tool for many parts of contemporary mathematics and physics. In this method, all variables in equations used are bounded of order one (Krantz. 2007, 3-12). This means that the magnitude of the dimensionless variables created are between zero and one. Generally an increase in their magnitude indicates an increase in their significance.

Also, one can determine what factors could be altered without a high impact change in the entire process. The procedure that involves the scaling of mathematical models is explained in the book referenced for both dimensional and dimensionless variables, the steps for dimensionless variables used in this work are also listed below (Krantz. 2007).

1. Write the describing equations, initial and boundary conditions for the process
2. Define unspecified scale factors for all variables in both the equations and conditions.
3. Also define unspecified reference factors for variables not referenced to zero
4. Form dimensionless variables by rearranging the scale and reference factors created
5. Introduce these dimensionless variables into the describing equations and their initial and boundary conditions.

6. Divide the equations and conditions through by the coefficient of one term that would be retained in every equation
7. Check that the principal terms in the equations are bounded by the order of one and check procedure for errors.

It is important to note that the group of variables in the equations formed after step six are pi groups and provide a lot of information on the relationship between the individual variables and the overall process. These pi groups can be verified for independence using MATLAB to eliminate repetitions. An extensive example on the utilization of the scaling analysis procedure to form dimensionless groups can be seen in Moghanloo (2012).

3.3.1 Formation of pi groups from deposition model

The idea behind the scaling analysis is the substitution of independent and dependent variables with in governing equations with terms that are dimensionless. The process yields insight to the relationships that exist between the parameters and describing variables and all these is realized without mathematically solving the equations describing the process in question.

This scaling analysis methodology was utilized for both processes described in this work; Asphaltene deposition in porous media and also in the wellbore. The 21 dimensionless groups discussed in the following chapter were realized from this process after the scaling analysis had been conducted. In this subsection, the mathematical formulation of the pi groups is shown in steps to create an understanding of how the pi groups were realized starting with deposition in porous media and then in the wellbore.

The describing equations for asphaltene deposition in porous media are as follows;

Mass balance equations

$$\frac{\partial}{\partial t}(\phi \rho_v w_{OL}) + \frac{\partial}{\partial x}(\rho_L u_L w_{OL}) = 0 \tag{3.3}$$

$$\frac{\partial}{\partial t}(\phi C_A \rho_A + \phi \rho_L w_{AL}) + \frac{\partial}{\partial x}(\rho_L u_L w_{SAL} + \rho_L u_L w_{AL}) = -\rho_A \frac{\partial E_A}{\partial t} \tag{3.4}$$

Asphaltene Deposition Model

$$\frac{\partial E_A}{\partial t} = \propto C_A \phi - \beta E_A \left(v_L - v_{cr,L}\right) + \gamma u_L \, C_A \tag{3.5}$$

Porosity Reduction Model

$$\phi = \phi_0 - E_A \tag{3.6}$$

Permeability Reduction Model

$$k = f_p k_0 \left(\frac{\phi}{\phi_0}\right)^3 \tag{3.7}$$

Momentum Balance Equation

$$u_L = -\frac{k}{\mu_L}\frac{\partial P}{\partial x} \tag{3.8}$$

The next step in the scaling analysis process is to define a scale factor for each of the variables in the equation, including variables in the boundary and initial conditions. This scale factor is described based on a reference factor also described for each equation. After that, the initial variable is then defined by these scale and reference factors. The scale factors defined and the new definition of the variables are shown below;

$$t_s = \frac{t}{t_r} \; ; t = t_s t_r \tag{3.9}$$

$$\phi_s = \frac{\phi}{\phi_r} \; ; \; \phi = \phi_s \phi_r \tag{3.10}$$

$$\rho_{v_s} = \frac{\rho_v}{\rho_{v_r}} \; ; \; \rho_v = \rho_{v_s} \rho_{v_r} \tag{3.11}$$

$$w_{OL_s} = \frac{w_{OL}}{w_{OL_r}} \; ; \; w_{OL} = w_{OL_s} w_{OL_r} \tag{3.12}$$

$$x_s = \frac{x}{x_r} \; ; \; x = x_s x_r \tag{3.13}$$

$$\rho_{L_s} = \frac{\rho_L}{\rho_{L_r}} \; ; \; \rho_L = \rho_{L_s}\rho_{L_r} \tag{3.14}$$

$$u_{L_s} = \frac{u_L}{u_{L_r}} \; ; \; u_L = u_{L_s}u_{L_r} \tag{3.15}$$

$$C_{A_s} = \frac{C_A}{C_{A_r}} \; ; \; C_A = C_{A_s}C_{A_r} \tag{3.16}$$

$$\rho_{A_s} = \frac{\rho_A}{\rho_{A_r}} \; ; \; \rho_A = \; \rho_{A_s}\rho_{A_r} \tag{3.17}$$

$$w_{AL_s} = \frac{w_{AL}}{w_{AL_r}} \; ; \; w_{AL} = w_{AL_s}w_{AL_r} \tag{3.18}$$

$$E_{A_s} = \frac{E_A}{E_{A_r}} \; ; \; E_A = E_{A_s}E_{A_r} \tag{3.19}$$

$$v_{L_s} = \frac{v_L}{v_{L_r}} \; ; \; v_L = v_{L_s}v_{L_r} \tag{3.20}$$

$$k_s = \frac{k}{k_r} \; ; \; k = k_s k_r \tag{3.21}$$

$$k_{0_s} = \frac{k_0}{k_{0_r}} \; ; \; k_0 = k_{0_s}k_{0_r} \tag{3.22}$$

$$P_s = \frac{P}{P_r} \; ; P = P_s P_r \tag{3.23}$$

After the scale and reference factors have been defined for all equations, the variables are then replaced in the original equations by their definition in terms of these factors. The definitions are showed above and the new equations for the scale and reference factors are shown below. It is important to note that these steps are repeated for the initial and boundary conditions specific to the process described.

Mass balance equations

$$\frac{\partial}{\partial t_s t_r}\left(\phi_s\phi_r\rho_{v_s}\rho_{v_r}w_{OL_s}w_{OL_r}\right) + \frac{\partial}{\partial x_s x_r}\left(\rho_{L_s}\rho_{L_r}u_{L_s}u_{L_r}w_{OL_s}w_{OL_r}\right) = 0$$

$$\frac{\partial}{\partial t_s t_r}\left(\phi_s \phi_r C_{A_s} C_{A_r} \rho_{A_s} \rho_{A_r} + \phi_s \phi_r \rho_{L_s} \rho_{L_r} w_{AL_s} w_{AL_r}\right) +$$

$$\frac{\partial}{\partial x_s x_r}\left(\rho_{L_s} \rho_{L_r} u_{L_s} u_{L_r} w_{SAL_s} w_{SAL_r} + \rho_{L_s} \rho_{L_r} u_{L_s} u_{L_r} w_{AL_s} w_{AL_r}\right) = -\rho_{A_s} \rho_{A_r} \frac{\partial E_{A_s} E_{A_r}}{\partial t_s t_r}$$

Asphaltene Deposition Model

$$\frac{\partial E_{A_s} E_{A_r}}{\partial t_s t_r} = \propto C_{A_s} C_{A_r} \phi_s \phi_r - \beta E_{A_s} E_{A_r}\left(v_{L_s} v_{L_r} - v_{cr,L}\right) + \gamma u_{L_s} u_{L_r} C_{A_s} C_{A_r}$$

Porosity Reduction Model

$$\phi_s \phi_r = \phi_{0_s} \phi_{0_r} - E_{A_s} E_{A_r}$$

Permeability Reduction Model

$$k_s k_r = f_p k_{0_s} k_{0_r} \left(\frac{\phi_s \phi_r}{\phi_{0_s} \phi_{0\,r}}\right)^3$$

Momentum Balance Equation

$$u_{L_s} u_{L_r} = -\frac{k_s k_r}{\mu_{L_s} \mu_{L_r}} \frac{\partial P_s P_r}{\partial x_s x_r}$$

After introducing the scale and reference factors into the equation, the next step in the scaling process is to separate the scale factors from the variables in the equation. In this step what is done is a simple rearrangement without making significant changes to the definition of the equation. This would enable us to identify a term that would be utilized in the steps to follow. Which is the process of making the coefficient of one of the terms in each equation have a coefficient equal to one. To do this the equation is divided by

the coefficient of the term chosen to have the unity coefficient equivalence. Rearrangements of the equations are shown below for all six equations defining asphaltene deposition in the porous media. After this, the equations are re-written where a term is given the unity coefficient.

Mass balance equations

$$\frac{\phi_s \rho_{v_s} w_{OL_S}}{t_s} \frac{\partial}{\partial t_r} \left(\phi_r \rho_{v_r} w_{OL_r} \right) + \frac{\rho_{L_s} u_{L_s} w_{OL_S}}{x_s} \frac{\partial}{\partial x_r} \left(\rho_{L_r} u_{L_r} w_{OL_r} \right) = 0$$

$$\frac{\phi_s C_{A_S} \rho_{A_S}}{t_s} \frac{\partial}{\partial t_r} \phi_r C_{A_r} \rho_{A_r} + \frac{\phi_s \rho_{L_s} w_{AL_S}}{t_s} \frac{\partial}{\partial t_r} \phi_r \rho_{L_r} w_{AL_r} + \frac{\rho_{L_s} u_{L_s} w_{SAL_s}}{x_s} \frac{\partial}{\partial x_r} \rho_{L_r} u_{L_r} w_{SAL_r} +$$

$$\frac{\rho_{L_s} u_{L_s} w_{AL_s}}{x_s} \frac{\partial}{\partial x_r} \rho_{L_r} u_{L_r} w_{AL_r} = -\rho_{A_s} \frac{E_{AS}}{t_s} \rho_{A_r} \frac{\partial E_{A_r}}{\partial t_r}$$

Asphaltene Deposition Model

$$\frac{E_{AS}}{t_s} \frac{\partial E_{A_r}}{\partial t_r} = \propto C_{A_s} \phi_s C_{A_r} \phi_r - \beta E_{A_s} v_{L_s} E_{A_r} \left(v_{L_r} - v_{cr,L} \right) + \gamma u_{L_s} C_{A_s} u_{L_r} C_{A_r}$$

Porosity Reduction Model

$$\phi_s \phi_r = \phi_{0_s} \phi_{0_r} - E_{A_s} E_{A_r}$$

Permeability Reduction Model

$$k_s k_r = f_p k_{0_s} k_{0_r} \left(\frac{\phi_s \phi_r}{\phi_{0_s} \phi_{0\,r}} \right)^3$$

Momentum Balance Equation

$$u_{L_s}u_{L_r} = -\frac{k_s k_r}{\mu_{L_s}\mu_{L_r}}\frac{P_s}{x_s}\frac{\partial P_r}{\partial x_r}$$

The equations are then re-written as discussed to account for the change in coefficient to represent an analysis bounded by the order of one. At this point the pi groups are easily identifiable and are shown in the final step.

Mass balance equations

$$\frac{\partial}{\partial t_r}\left(\phi_r \rho_{v_r} w_{OL_r}\right) + \frac{t_s u_{L_s}}{\phi_s x_s}\frac{\partial}{\partial x_r}\left(\rho_{L_r} u_{L_r} w_{OL_r}\right) = 0$$

$$\frac{\partial}{\partial t_r}\phi_r C_{A_r}\rho_{A_r} + \frac{w_{AL_S}}{C_{A_S}}\frac{\partial}{\partial t_r}\phi_r \rho_{L_r} w_{AL_r} + \frac{t_s u_{L_s} w_{SAL_S}}{\phi_s C_{A_S} x_s}\frac{\partial}{\partial x_r}\rho_{L_r} u_{L_r} w_{SAL_r} +$$

$$\frac{t_s u_{L_s} w_{AL_S}}{\phi_s C_{A_S} x_s}\frac{\partial}{\partial x_r}\rho_{L_r} u_{L_r} w_{AL_r} = -\frac{E_{A_S}}{\phi_s C_{A_S}}\rho_{A_r}\frac{\partial E_{A_r}}{\partial t_r}$$

Asphaltene Deposition Model

$$\frac{1}{\beta v_{L_s} t_s}\frac{\partial E_{A_r}}{\partial t_r} = \frac{\propto C_{A_S}\phi_s}{\beta E_{A_S} v_{L_S}} C_{A_r}\phi_r - E_{A_r}\left(v_{L_r} - v_{cr,L}\right) + \frac{\gamma u_{L_s} C_{A_S}}{\beta E_{A_S} v_{L_S}} u_{L_r}\, C_{A_r}$$

Porosity Reduction Model

$$\phi_r = \frac{\phi_{0_S}}{\phi_s}\phi_{0_r} - \frac{E_{A_S}}{\phi_s}E_{A_r}$$

Permeability Reduction Model

$$k_r = \frac{f_p k_{0_S}}{k_s} k_{0_r} \frac{1}{k_s^3}\left(\frac{\phi_s \phi_r}{\phi_{0_S}\phi_{0\,r}}\right)^3$$

Momentum Balance Equation

$$u_{L_r} = -\frac{k_s k_r}{\mu_{L_s}\mu_{L_r}u_{L_s}}\frac{P_s}{x_s u_{L_s}}\frac{\partial P_r}{\partial x_r}$$

The pi groups realized are then placed in brackets these are the pi groups shown for porous media in chapter 4. Some of them may be rearranged for easy interpretation however what they represent remain unchanged.

Mass balance equations

$$\frac{\partial}{\partial t_r}\left(\phi_r \rho_{v_r} w_{OL_r}\right) + \left[\frac{t_s u_{L_s}}{\phi_s x_s}\right]\frac{\partial}{\partial x_r}\left(\rho_{L_r} u_{L_r} w_{OL_r}\right) = 0$$

$$\frac{\partial}{\partial t_r}\phi_r C_{A_r}\rho_{A_r} + \left[\frac{w_{AL_s}}{C_{A_s}}\right]\frac{\partial}{\partial t_r}\phi_r \rho_{L_r} w_{AL_r} + \left[\frac{t_s u_{L_s} w_{SAL_s}}{\phi_s C_{A_s} x_s}\right]\frac{\partial}{\partial x_r}\rho_{L_r} u_{L_r} w_{SAL_r} +$$

$$\left[\frac{t_s u_{L_s} w_{AL_s}}{\phi_s C_{A_s} x_s}\right]\frac{\partial}{\partial x_r}\rho_{L_r} u_{L_r} w_{AL_r} = -\left[\frac{E_{AS}}{\phi_s C_{A_s}}\right]\rho_{A_r}\frac{\partial E_{A_r}}{\partial t_r}$$

Asphaltene Deposition Model

$$\left[\frac{1}{\beta v_{L_s} t_s}\right]\frac{\partial E_{A_r}}{\partial t_r} = \left[\frac{\propto C_{A_s}\phi_s}{\beta E_{A_s} v_{L_s}}\right] C_{A_r}\phi_r - E_{A_r}\left(v_{L_r} - v_{cr,L}\right) + \left[\frac{\gamma u_{L_s} C_{A_s}}{\beta E_{A_s} v_{L_s}}\right] u_{L_r}\, C_{A_r}$$

Porosity Reduction Model

$$\phi_r = \left[\frac{\phi_{0_s}}{\phi_s}\right]\phi_{0_r} - \left[\frac{E_{A_s}}{\phi_s}\right] E_{A_r}$$

Permeability Reduction Model

$$k_r = \left[\frac{f_p k_{0_s}}{k_s}\right] k_{0_r}\left[\frac{1}{k_s^3}\right]\left(\frac{\phi_s \phi_r}{\phi_{0_s}\phi_{0\,r}}\right)^3$$

Momentum Balance Equation

$$u_{L_r} = -\left[\frac{k_s}{\mu_{L_S} u_{L_S}} \frac{P_s}{x_s}\right] \frac{k_r}{\mu_{L_r}} \frac{\partial P_r}{\partial x_r}$$

Now that the pi groups have been realized for asphaltene deposition in porous media, the scaling analysis methodology will also be utilized to find the pi groups related to asphaltene deposition in pipes and wellbores. Starting with the describing equations. The describing equations for asphaltene deposition in porous media are as follows;

Mass Balance Equations

Solid Asphaltene in stream:

$$\frac{\partial}{\partial t}(A\rho_o \propto_o + Ac_a \propto_o) + \frac{\partial}{\partial x}(A\rho_o \propto_o u_o + Au_o c_a) = A(\varphi_o + \gamma_a - m_{da}) \quad (3.24)$$

Oil in liquid phase:

$$\frac{\partial}{\partial t}(\rho_o \propto_o) + \frac{1}{A}\frac{\partial}{\partial x}(A\rho_o \propto_o u_o) = \varphi_o \quad (3.25)$$

Cleaver and Yates deposition model definition

$$N = \frac{0.084 \Delta C V_{avg} \sqrt{f/2}}{Sc^{2/3}} \quad (3.26)$$

$where\ \Delta C = C_b - C_s$

Rate of Asphaltene attachment

$$m_{da} = \frac{\partial}{\partial x} SP(N) \quad (3.27)$$

Momentum Balance Equation

$$\frac{\partial}{\partial t}(\rho_o u_o) + \frac{\partial}{\partial x}(\rho_o u_o^2) + (144.0 g_c)\frac{\partial P}{\partial x} + \rho_0 g sin\theta + \frac{\tau_o \pi D}{A} = 0 \quad (3.28)$$

As with the deposition equations for porous media, the next step in the scaling analysis process is to define a scale factor for each of the variables in the equation, including variables in the boundary and initial conditions. The scale factors defined and the new definition of the variables are shown below;

$$t_s = \frac{t}{t_r} \; ; t = t_s t_r \tag{3.29}$$

$$A_S = \frac{A}{A_r} \; ; A = A_s A_r \tag{3.30}$$

$$\rho_{o_S} = \frac{\rho_o}{\rho_{o_r}} \; ; \; \rho_o = \rho_{o_S} \rho_{o_r} \tag{3.31}$$

$$\propto_{o_S} = \frac{\propto_o}{\propto_{o_r}} \; ; \; \propto_o = \propto_{o_S} \propto_{o_r} \tag{3.32}$$

$$c_{a_S} = \frac{c_a}{c_{a_r}} \; ; \; c_a = c_{a_S} c_{a_r} \tag{3.33}$$

$$x_s = \frac{x}{x_r} \; ; \; x = x_s x_r \tag{3.34}$$

$$u_{o_S} = \frac{u_o}{u_{o_r}} \; ; \; u_o = u_{o_S} u_{o_r} \tag{3.35}$$

$$\varphi_{o_S} = \frac{\varphi_o}{\varphi_{o_r}} \; ; \; \varphi_o = \varphi_{o_S} \varphi_{o_r} \tag{3.36}$$

$$\gamma_{a_S} = \frac{\gamma_a}{\gamma_{a_r}} \; ; \; \gamma_a = \gamma_{a_S} \gamma_{a_r} \tag{3.37}$$

$$m_{da_S} = \frac{m_{da}}{m_{da_r}} \; ; \; m_{da} = m_{da_S} m_{da_r} \tag{3.38}$$

$$P_s = \frac{P}{P_r} \; ; P = P_s P_r \tag{3.39}$$

$$\tau_{o_S} = \frac{\tau_o}{\tau_{o_r}} \; ; \; \tau_o = \tau_{o_S} \tau_{o_r} \tag{3.40}$$

After the scale and reference factors have been defined for all equations, the variables are then replaced in the original equations by their definition in terns of these factors. The new equations for the scale and reference factors are shown below.

Mass Balance Equations

Solid Asphaltene in stream:

$$\frac{\partial}{\partial t_s t_r}\left(A_s A_r \rho_{o_s}\rho_{o_r} \propto_{o_s}\propto_{o_r} + A_s A_r c_{a_s} c_{a_r} \propto_{o_s}\propto_{o_r}\right) +$$

$$\frac{\partial}{\partial x_s x_r}\left(A_s A_r \rho_{o_s}\rho_{o_r} \propto_{o_s}\propto_{o_r} u_{o_s} u_{o_r} + A_s A_r u_{o_s} u_{o_r} c_{a_s} c_{a_r}\right) = A_s A_r(\varphi_{o_s}\varphi_{o_r} + \gamma_{a_s}\gamma_{a_r} - m_{da_s} m_{da_r})$$

Oil in liquid phase:

$$\frac{\partial}{\partial t_s t_r}\left(\rho_{o_s}\rho_{o_r} \propto_{o_s}\propto_{o_r}\right) + \frac{1}{A_s A_r}\frac{\partial}{\partial x_s x_r}\left(A_s A_r \rho_{o_s}\rho_{o_r} \propto_{o_s}\propto_{o_r} u_{o_s} u_{o_r}\right) = \varphi_{o_s}\varphi_{o_r}$$

Cleaver and Yates deposition model definition

$$N = \frac{0.084 \Delta C V_{avg}\sqrt{f/2}}{Sc^{2/3}}$$

$where\ \Delta C = C_b - C_s$

Rate of Asphaltene attachment

$$m_{da_s} m_{da_r} = \frac{\partial}{\partial x_s x_r} SP(N)$$

Momentum Balance Equation

$$\frac{\partial}{\partial t_s t_r}\left(\rho_{o_s}\rho_{o_r} u_{o_s} u_{o_r}\right) + \frac{\partial}{\partial x_s x_r}\left(\rho_{o_s}\rho_{o_r} u_{o_s}^2 u_{o_r}^2\right) + (144.0 g_c)\frac{\partial P_s P_r}{\partial x_s x_r} +$$

$$\rho_{o_s}\rho_{o_r} g sin\theta + \frac{\tau_{o_s}\tau_{o_r}\pi D}{A_s A_r} = 0$$

The scale factors are then separated from the reference factors as was done with the deposition equations for porous media, to enable one come up with the pi groups associated with the process.

Mass Balance Equations

Solid Asphaltene in stream:

$$\frac{A_s \rho_{o_s} \propto_{o_s}}{t_s} \frac{\partial}{\partial t_r} A_r \rho_{o_r} \propto_{o_r} + \frac{A_s c_{a_s} \propto_{o_s}}{t_s} \frac{\partial}{\partial t_r} A_r c_{a_r} \propto_{o_r} +$$

$$\frac{A_s \rho_{o_s} \propto_{o_s} u_{o_s}}{x_s} \frac{\partial}{\partial x_r} A_r \rho_{o_r} \propto_{o_r} u_{o_r} + \frac{A_s c_{a_s} u_{o_s}}{x_s} \frac{\partial}{\partial x_r} A_r u_{o_r} c_{a_r} = A_s \varphi_{o_s} A_r \varphi_{o_r} + A_s \gamma_{a_s} A_r \gamma_{a_r} -$$

$$A_s m_{da_s} A_r m_{da_r}$$

Oil in liquid phase:

$$\frac{\rho_{o_s} \propto_{o_s}}{t_s} \frac{\partial}{\partial t_r} \left(\rho_{o_r} \propto_{o_r} \right) + \frac{\rho_{o_s} \propto_{o_s} u_{o_s}}{x_s} \frac{1}{A_r} \frac{\partial}{\partial x_r} \left(A_r \rho_{o_r} \propto_{o_r} u_{o_r} \right) = \varphi_{o_s} \varphi_{o_r}$$

Cleaver and Yates deposition model definition

$$N = \frac{0.084 \Delta C V_{avg} \sqrt{f/2}}{Sc^{2/3}}$$

$$where\ \Delta C = C_b - C_s$$

Rate of Asphaltene attachment

$$m_{da_s} m_{da_r} = \frac{1}{x_s} \frac{\partial}{\partial x_r} SP(N)$$

Momentum Balance Equation

$$\frac{\rho_{o_s} u_{o_s}}{t_s} \frac{\partial}{\partial t_r} \left(\rho_{o_r} u_{o_r} \right) + \frac{\rho_{o_s} u_{o_s}^2}{x_s} \frac{\partial}{\partial x_r} \left(\rho_{o_r} u_{o_r}^2 \right) + \frac{P_s}{x_s} (144.0 g_c) \frac{\partial P_r}{\partial x_r} + \rho_{o_s} \rho_{o_r} g sin\theta +$$

$$\frac{\tau_{o_s}}{A_s} \frac{\tau_{o_r} \pi D}{A_r} = 0$$

To ensure that the pi groups are bounded by the order of one, the scalar groups are then divided by the coefficient of one of the terms in each equation. Finally the pi groups are then identified.

Mass Balance Equations

Solid Asphaltene in stream:

$$\frac{\partial}{\partial t_r} A_r \rho_{o_r} \propto_{o_r} + \frac{c_{a_s}}{\rho_{o_s}} \frac{\partial}{\partial t_r} A_r c_{a_r} \propto_{o_r} + \frac{t_s u_{o_s}}{x_s} \frac{\partial}{\partial x_r} A_r \rho_{o_r} \propto_{o_r} u_{o_r} +$$

$$\frac{t_s c_{a_s} u_{o_s}}{\rho_{o_s} \propto_{o_s} x_s} \frac{\partial}{\partial x_r} A_r u_{o_r} c_{a_r} = \frac{t_s \varphi_{o_s}}{\rho_{o_s} \propto_{o_s}} A_r \varphi_{o_r} + \frac{t_s}{\rho_{o_s} \propto_{o_s}} \gamma_{a_s} A_r \gamma_{a_r} - \frac{t_s m_{da_s}}{\rho_{o_s} \propto_{o_s}} A_r \, {}_s m_{da_r}$$

Oil in liquid phase:

$$\frac{\partial}{\partial t_r} \left(\rho_{o_r} \propto_{o_r} \right) + \frac{t_s u_{o_s}}{x_s} \frac{1}{A_r} \frac{\partial}{\partial x_r} \left(A_r \rho_{o_r} \propto_{o_r} u_{o_r} \right) = \frac{t_s \varphi_{o_s}}{\rho_{o_s} \propto_{o_s}} \varphi_{o_r}$$

Cleaver and Yates deposition model definition

$$N = \frac{0.084 \Delta C V_{avg} \sqrt{f/2}}{Sc^{2/3}}$$

$where\ \Delta C = C_b - C_s$

Rate of Asphaltene attachment

$$m_{da_r} = \frac{1}{m_{da_s} x_s} \frac{\partial}{\partial x_r} SP(N)$$

Momentum Balance Equation

$$\frac{\rho_{o_s} u_{o_s}}{t_s} \frac{\partial}{\partial t_r} \left(\rho_{o_r} u_{o_r} \right) + \frac{t_s u_{o_s}}{x_s} \frac{\partial}{\partial x_r} \left(\rho_{o_r} u_{o_r}^2 \right) + \frac{t_s P_s}{\rho_{o_s} u_{o_s} x_s} (144.0 g_c) \frac{\partial P_r}{\partial x_r} +$$

$$\frac{t_s}{u_{o_s}} \rho_{o_r} g sin\theta + \frac{\frac{\rho_{o_s} u_{o_s}}{t_s} \tau_{o_s}}{A_s} \frac{\tau_{o_r} \pi D}{A_r} = 0$$

The pi groups are then identified in brackets.

Mass Balance Equations

Solid Asphaltene in stream:

$$\frac{A_s\rho_{o_s}\propto_{o_s}}{t_s}\ \frac{\partial}{\partial t_r}A_r\rho_{o_r}\propto_{o_r}+\frac{A_sc_{a_s}\propto_{o_s}}{t_s}\ \frac{\partial}{\partial t_r}\ \ A_rc_{a_r}\propto_{o_r}+$$

$$\frac{A_s\rho_{o_s}\propto_{o_s}u_{o_s}}{x_s}\frac{\partial}{\partial x_r}A_r\rho_{o_r}\propto_{o_r}u_{o_r}+\frac{A_sc_{a_s}u_{o_s}}{x_s}\frac{\partial}{\partial x_r}A_ru_{o_r}c_{a_r}=A_s\varphi_{o_s}A_r\varphi_{o_r}+A_s\gamma_{a_s}A_r\gamma_{a_r}-$$

$$A_sm_{da_s}A_rm_{da_r}$$

Oil in liquid phase:

$$\frac{\rho_{o_s}\propto_{o_s}}{t_s}\ \frac{\partial}{\partial t_r}\left(\rho_{o_r}\propto_{o_r}\right)+\frac{\rho_{o_s}\propto_{o_s}u_{o_s}}{x_s}\frac{1}{A_r}\frac{\partial}{\partial x_r}\left(A_r\rho_{o_r}\propto_{o_r}u_{o_r}\right)=\varphi_{o_s}\varphi_{o_r}$$

Cleaver and Yates deposition model definition

$$N=\frac{0.084\Delta CV_{avg}\sqrt{f/2}}{Sc^{2/3}}$$

$$where\ \Delta C=C_b-C_s$$

Rate of Asphaltene attachment

$$m_{da_s}m_{da_r}=\frac{1}{x_s}\frac{\partial}{\partial x_r}SP(N)$$

Momentum Balance Equation

$$\frac{\rho_{o_s}u_{o_s}}{t_s}\frac{\partial}{\partial t_r}\left(\rho_{o_r}u_{o_r}\right)+\frac{\rho_{o_s}u_{o_s}^2}{x_s}\frac{\partial}{\partial x_r}\left(\rho_{o_r}u_{o_r}^2\right)+\frac{P_s}{x_s}(144.0g_c)\frac{\partial P_r}{\partial x_r}+\rho_{o_s}\rho_{o_r}gsin\theta+$$

$$\frac{\tau_{o_s}}{A_s}\frac{\tau_{o_r}\pi D}{A_r}=0$$

To ensure that the pi groups are bounded by the order of one, the scalar groups are then divided by the coefficient of one of the terms in each equation. Finally the pi groups are then identified.

Mass Balance Equations

Solid Asphaltene in stream:

$$\frac{\partial}{\partial t_r} A_r \rho_{o_r} \propto_{o_r} + \left[\frac{c_{a_s}}{\rho_{o_s}} \frac{\partial}{\partial t_r}\right] A_r c_{a_r} \propto_{o_r} + \left[\frac{t_s u_{o_s}}{x_s}\right] \frac{\partial}{\partial x_r} A_r \rho_{o_r} \propto_{o_r} u_{o_r} +$$

$$\left[\frac{t_s c_{a_s} u_{o_s}}{\rho_{o_s} \propto_{o_s} x_s}\right] \frac{\partial}{\partial x_r} A_r u_{o_r} c_{a_r} = \left[\frac{t_s \varphi_{o_s}}{\rho_{o_s} \propto_{o_s}}\right] A_r \varphi_{o_r} + \left[\frac{t_s}{\rho_{o_s} \propto_{o_s}} \gamma_{a_s}\right] A_r \gamma_{a_r} - \left[\frac{t_s m_{da_s}}{\rho_{o_s} \propto_{o_s}}\right] A_r \; m_{da_r}$$

Oil in liquid phase:

$$\frac{\partial}{\partial t_r}\left(\rho_{o_r} \propto_{o_r}\right) + \left[\frac{t_s u_{o_s}}{x_s}\right] \frac{1}{A_r} \frac{\partial}{\partial x_r}\left(A_r \rho_{o_r} \propto_{o_r} u_{o_r}\right) = \left[\frac{t_s \varphi_{o_s}}{\rho_{o_s} \propto_{o_s}}\right] \varphi_{o_r}$$

Cleaver and Yates deposition model definition

$$N = \frac{0.084 \Delta C V_{avg} \sqrt{f/2}}{Sc^{2/3}}$$

$where\ \Delta C = C_b - C_s$

Rate of Asphaltene attachment

$$m_{da_r} = \left[\frac{1}{m_{da_s} x_s}\right] \frac{\partial}{\partial x_r} SP(N)$$

Momentum Balance Equation

$$\frac{\partial}{\partial t_r}\left(\rho_{o_r} u_{o_r}\right) + \left[\frac{t_s u_{o_s}}{x_s}\right] \frac{\partial}{\partial x_r}\left(\rho_{o_r} u_{o_r}^2\right) + \left[\frac{t_s P_s}{\rho_{o_s} u_{o_s} x_s}\right] (144.0 g_c) \frac{\partial P_r}{\partial x_r} +$$

$$\left[\frac{t_s}{u_{o_s}}\right] \rho_{o_r} g sin\theta + \left[\frac{\frac{\rho_{o_s} u_{o_s}}{t_s} \tau_{o_s}}{A_s}\right] \frac{\tau_{o_r} \pi D}{A_r} = 0$$

All the pi groups attained from the scaling procedure are shown in the brackets for deposition in both porous media and wellbore. For deposition in the wellbore it is important to note that the dimensions of $\alpha = T^{-1}$; $\beta = L^{-1}$ and $\gamma = L^{-1}$ MATLAB was utilized to find the rank of the coefficient matrix in order to eradicate independence for both processes and the resulting pi groups are shown in Chapter 4.

Chapter 4: Scaling Analysis – Results and Discussion

The results obtained from the scaling analysis of the equations described in Chapter 3 are shown here and also analyzed. In this chapter, we start from results obtained from the scaling analysis for both pipe deposition and deposition in porous media. Then, results for the deposition in porous media is analyzed and finally deposition in pipes is equally analyzed. Results focus on specific pi groups obtained from the scaling analysis.

4.1 Pi groups obtained from scaling analysis of the deposition equations

The scaling analysis procedure resulted in the formation of dimensionless pi groups with an order of one magnitude after the constant numerical values are inputted. Thirteen pi groups were obtained for the deposition process in the porous media near the wellbore and are presented as pi groups 1 through 13. For asphaltene deposition in pipes, eight dimensionless pi groups were obtained from the scaling analysis procedure presented as pi groups 14 through 21. All pi groups are listed in Table 4.1.

Since all pi groups are bounded by an order of one magnitude, they can only be have values between zero and one. A value equal to zero indicates that the variables, for which the pi group is a coefficient, is not relevant to asphaltene deposition. A pi group equal to one shows highest level of significance for the deposition process for a given scenario. Based on data specific to any formation being considered the significance of the pi groups can also be determined as a unit.

Table 4.1 Pi groups obtained from scaling analysis of the asphaltene deposition models in porous media near the wellbore and also in pipes. $\pi_1 - \pi_{13}$ were obtained from porous media deposition while $\pi_{14} - \pi_{21}$ were from pipe deposition.

$Pi\ number$	$Defining\ dimensionless\ group$
π_1	$\frac{t\rho_L u_L}{x\rho_v \phi}$
π_2	$\frac{\rho_L w_{AL}}{C_A \rho_A}$
π_3	$\frac{t\rho_L u_L w_{SAL}}{x\phi C_A \rho_A}$
π_4	$\frac{t\rho_L u_L w_{AL}}{x\phi C_A \rho_A}$
π_5	$\frac{E_A}{\phi C_A}$
π_6	$\frac{1}{\phi}$
π_7	$\frac{E_A}{\phi}$
π_8	$f_p \frac{\phi}{k}$
π_9	$\frac{kp}{\mu_L x u_L}$
π_{10}	$\frac{\alpha C_A \phi}{\beta E_A \Delta v}$
π_{11}	$\frac{1}{t\Delta v \beta}$
π_{12}	$\frac{\gamma C_A u_L}{\beta E_A \Delta v}$

π_{13}	$\frac{L}{x}$
π_{14}	$\frac{c_a}{\rho_0 \alpha_0}$
π_{15}	$\frac{x}{t u_0}$
π_{16}	$\frac{t \rho_0 u_0}{x c_a}$
π_{17}	$\frac{x \varphi_0}{\rho_0 \alpha_0 u_0}$
π_{18}	$\frac{x \gamma_a}{\rho_0 \alpha_0 u_0}$
π_{19}	$\frac{x m_{da}}{\rho_0 \alpha_0 u_0}$
π_{20}	$\frac{t \varphi_0}{\rho_0 \alpha_0}$
π_{21}	$\frac{SpN}{m_{da} x}$

4.2 Analysis of results from deposition in porous media

For asphaltene deposition in the porous media π_{10}, π_{11} and π_{12} were obtained specifically from the asphaltene deposition equation in 3.1 in chapter 3. The pi groups can be justified based on scenarios creating simplifications to Equation 3.1. Equation 4.1 shows the deposition equation in its scaled form with the associated pi groups. In very low porosity formation, π_{10} would veer towards zero. The surface deposition term which multiplies this pi group would be negligible and the asphaltene deposition would

only depend on entrainment and the rate of pore throat plugging as shown in equation 4.2.

This is an example of an obvious conclusion that can be verified with scaling analysis. If the porosity in a formation is very low, it is expected that the deposition of asphaltene would be driven by pore blockage, the positive term in equation in 4.1. It is also important to note that an increase in C_A would cause an increase in the overall deposition rate, since the asphaltene concentration term is also important for the rate of pore throat plugging.

$$\left[\frac{1}{t\Delta v\beta}\right]\frac{\partial E_A}{\partial t} = \left[\frac{\alpha C_A \phi}{\beta E_A \Delta v}\right] C_A\phi - E_A\left(v_L - v_{cr,L}\right) + \left[\frac{\gamma C_A u_L}{\beta E_A \Delta v}\right] u_L\, C_A \tag{4.1}$$

$$\frac{\partial E_A}{\partial t} = \gamma u_L\, C_A - \beta E_A\left(v_L - v_{cr,L}\right) \tag{4.2}$$

When $v_{cr,L}$, critical interstitial velocity of the liquid phase is greater than the interstitial velocity v_L, the entrainment rate coefficient β, is equal to zero. In this case, the deposition would be driven by surface deposition and pore throat plugging rate, as π_{11} and π_{12} would both get infinitely large in Equation 4.1. For all the pi groups discussed, decreasing the entrainment rate coefficient would increase the rate of asphaltene deposition since the entrainment of the solid particles in the fluid bulk abates the deposition of these particles. A decrease in the difference between the interstitial velocities would have similar effects as well. When both scenarios are combined, low porosity formation and insignificant entrainment, the deposition equation is further simplified to equation 4.3.

$$\frac{\partial E_A}{\partial t} = \propto C_A\phi \tag{4.3}$$

Here, the deposition is solely driven by the rate of surface deposition. Based on the original Equation 3.1 alone, one would assume that the deposition would be driven by the rate of pore throat plugging. Scaling analysis performed in Equation 4.1 shows the relationship between entrainment and pore throat plugging. An increase in the entrainment rate constant would cause a significant decrease in the rate of pore throat plugging, reducing its effects on the overall deposition.

For this scenario the rate of surface deposition, shown in Equation 4.3, would depend on the relative magnitude of porosity ϕ and the entrainment constant $\beta \; in \; \pi_{10}$. For other cases where the entrainment rate coefficient is not equal to zero, the interstitial velocity is greater than the critical interstitial velocity of the fluid. From the original Equation 3.1, it is important to keep the critical interstitial velocity as low as possible in order to increase the velocity difference and decrease the resulting asphaltene deposition.

4.3 Analysis of results from deposition in pipes and wellbores

The major equation describing asphaltene deposition in the wellbore and pipes is presented as Equation 3.2 in chapter 3. One of the pi groups obtained from the defining equations, π_{16}, is a function of the time, density, fluid velocity, length of wellbore and asphaltene concentration in the crude oil. It is shown in Equation 4.4 and again in Table 4.1. Figure 4.1 shows a speculative description of the relationship expected from the individual factors that make up the π_{16} group and asphaltene deposition in pipes.

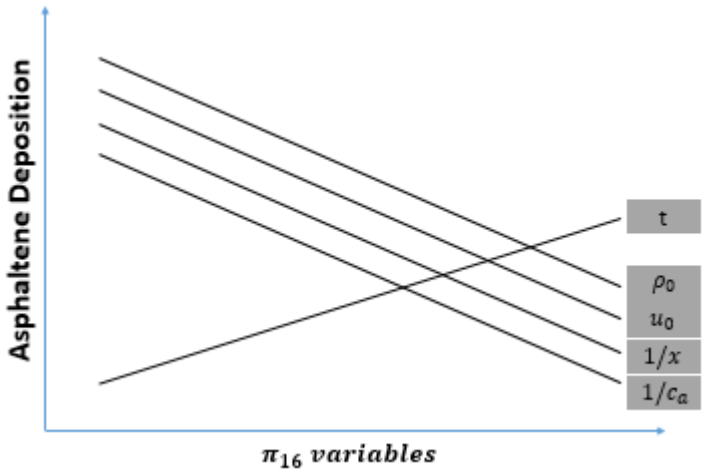

Figure 4.1 Graphical representation of the expected relationship between the variables constituting the pi group and asphaltene deposition

Again the graph shows the expected relationship between the variables in the pi group against asphaltene deposition. Due to an increase in the contact time between the flowing system and the pipe, an increase in the time should create an increase the total amount of asphaltene deposited. An increase in mixture density of the flowing system should cause a decrease in asphaltene deposition because increased density will cause increase stability and as a result there should be a reduction in the amount of asphaltene precipitating out of the solution.

If the velocity of the mixture is increased, the contact time of the flowing system and the pipe surface is reduced. As a result, the amount of asphaltene deposited in the pipe should equally reduce. Also, at increased velocity, there would be increased entrainment (refer to equation 3.2). This would cause the precipitated particles to remain in the flowing system, reducing the possibilities of the particles being dropped off as deposit on the pipe surface. If the pipe length is increased, there would be an

increase in the contact time between the flowing system and the pipe surface and as such the deposition should increase.

Finally, an increase in the concentration of asphaltene precipitate would increase the solid content in the flowing system and would result in an increased amount of deposition being experienced. Figure 4.2 shows the expected relationship between the pi group as a whole and asphaltene deposition. This speculation takes into account the effects of the individual factors that make up the pi group discussed above.

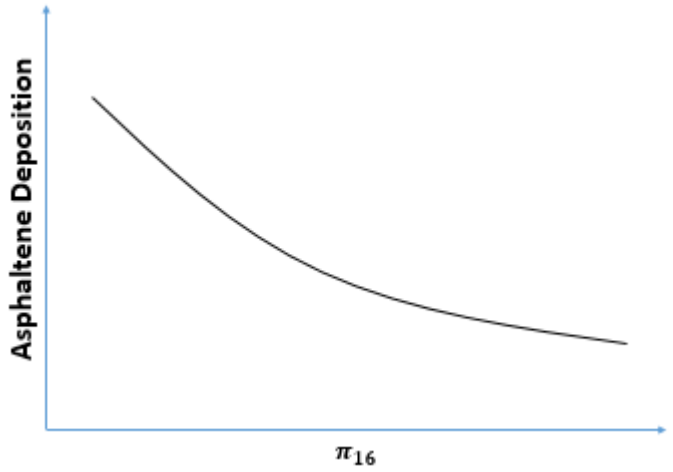

Figure 4.2 Graphical representation of the expected relationship between π_{16} and asphaltene deposition in pipes

Based on the speculative relationship presented in Figure 4.2, in order to reduce asphaltene deposition, it is important to make π_{16} as large as possible. An increase in the π_{16} would cause a decrease in the amount of asphaltene deposition experienced in pipes. π_{16} was also analyzed mathematically to create a better understanding of its description and potential role in asphaltene deposition. Figure 4.3 shows the description formulated in terms of an equation. Where $t_{exposure}$ is defined as the time the flowing system spends in contact with the walls of the pipes. It can be related to residence time. t_{travel} is the time it takes the flowing system to travel through the pipe in its entirety.

$$\pi_{16} = \frac{t\rho_0 u_0}{xc_a} = \frac{t}{\frac{x}{u_0}\frac{c_a}{\rho_0}} = \frac{t_{exposure}}{t_{travel}\left[\frac{Amount\ of\ present\ asphaltene}{Volume\ of\ flow\ system}\right]}$$

Figure 4.3 Mathematical description of the dimensionless π_{16}

4.3.1 Analysis of π_{16} against flowrate

The pi group was analyzed numerically based on experimental data obtained from Hashmi et al (2015) and Nabzar and Aguilera (2008). In the work done, a dimensionless time defined by Equation 4.5, was varied over a change in pressure drop to determine the onset of asphaltene deposition. Significant deposition was experienced at higher pressure drop values. These pressure drops were defined as difference in original and final pressure by Hashmini et al and as a ratio of final pressure to initial pressure by Nabzar and Aguilera. Figures from experimental data utilized are shown in Appendix C.

$$\pi_{16} = \frac{t\rho_0 u_0}{xc_a} \tag{4.4}$$

$$\tau = \frac{Qt}{V} \tag{4.5}$$

For the dimensionless time τ , Q is the flow rate, V is the volume of pipe and t is time in hours. At varied fluid velocities, the time it takes for significant asphaltene deposition was determined from Figures C-1 and C-2 in Appendix C, with the help of Equation 4.4. These values were then utilized to calculate the critical value of π_{16} above which asphaltene deposition is significant. Figures 4.4 and 4.5 show the graph of critical values of the dimensionless $\frac{\pi_{16}}{\rho_0}$ for different flow rates. It is important to note that the data sets could not be combined because varying assumptions were made during data collection on the representation of the pressure difference. Also, it is assumed that a

pressure difference of 0.2 and 1.2 constitutes significant deposition in Figures 4.4 and 4.5 respectively.

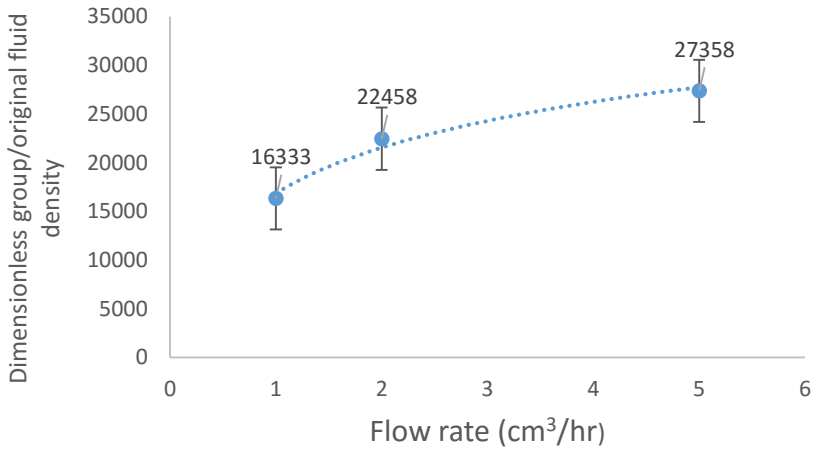

Figure 4.4. Critical values of dimensionless pi group obtained from scaling analysis above which significant deposition would occur. Assuming a change in pressure of 0.2 constitutes significant deposition. Experimental data obtained from Hashmi et al (2015).

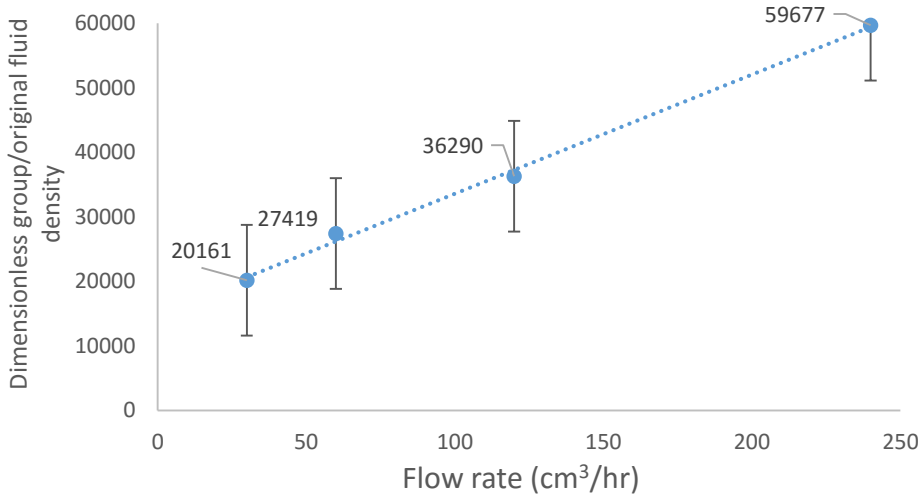

Figure 4.5. Critical values of dimensionless pi group obtained from scaling analysis above which significant deposition would occur. Assuming a change in pressure of 1.2 constitutes significant deposition. Experimental data obtained from Nabzar and Aguilera (2008).

The data points shown in Figures 4.4 and 4.5 were best fitted to a logarithmic and linear trend line respectively. The difference in fit may be as a result of the varied assumptions or could also imply that the trend becomes linear at increasing flow rates. In order to draw conclusions on the nature of the trend line for this dimensionless group, simulations could be used to verify the critical values obtained. Ten percent error bars were used to account for inaccuracies that may have occurred from reading values of dimensionless time from the plots in Appendix C.

In practice, results obtained from the numerical analysis of pi groups acquired by scaling analysis go a long way to determining optimum conditions that could be utilized in the field to prevent asphaltene deposition. Based on the trends observed for the pi group calculated against flow rate in Figures 4.4 and 4.5, it can be insinuated that a logarithmic trend exists between π_{16} and overall flow rate in the wellbore and pipes. Figures 4.6 and 4.7 show a graph and a schematic respectively explaining the overall trend based on the logarithmic trend line fitted to Figure 4.4. Deposition occurs below the logarithmic curve, therefore to prevent significant asphaltene deposition, the flow rate and calculated π_{16} group should be lie above the curve.

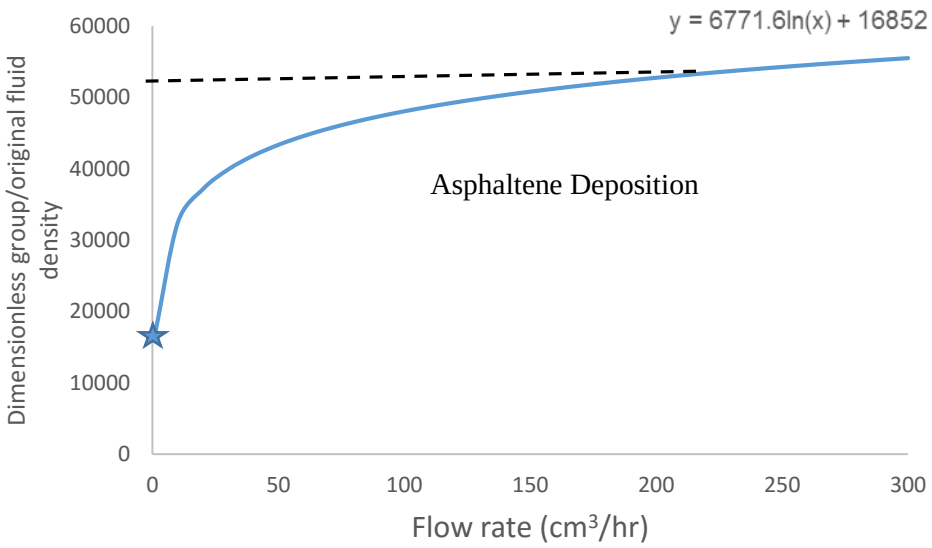

Figure 4.6. Graph showing the π_{16} relationship at varied flow rates. Above the curve, asphaltene deposition will occur. Above the curve, significant deposition does not occur.

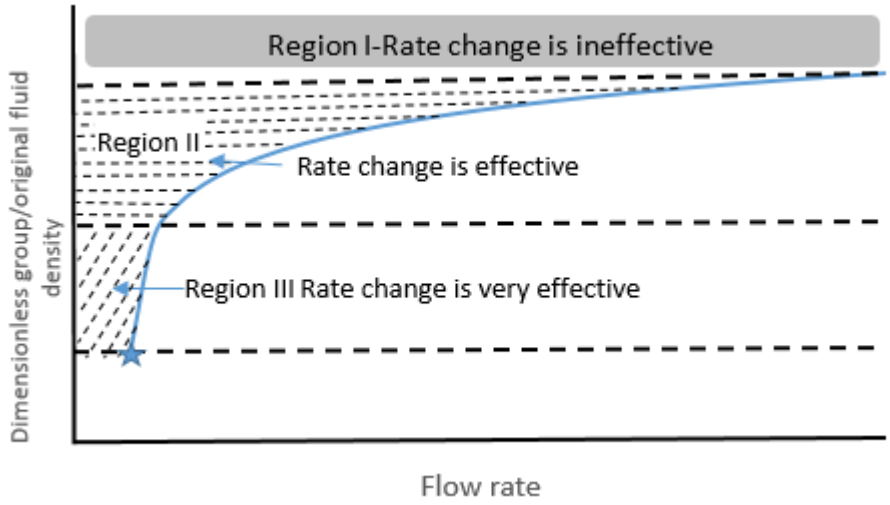

Figure 4.7. Schematic showing the general trend of the π_{16} relationship flow rates. Above the curve, asphaltene deposition will not occur, this is a safe zone. Below the curve, where there is no shading, significant deposition occurs. Regions I, II and III show the different conditions and how an increase in flowrate would affect deposition under these conditions.

Generally, an increase in the flow rate between 0 and 200 cm^3/hr would cause the downhole conditions to fall within the safe zone-above the graph. However, there exists a π_{16} value below which a decrease in the flow rate would have little to no effect on the mitigation of asphaltene deposition. Based on Figure 5, the value lies around 16852cm^3/kg from the equation and is shown in the graph by the star. There also exists a dimensionless value above which asphaltene deposition would not occur irrespective of the flow rate. This value is denoted by the dashed line in the graph and from the equation is 51000 cm^3/kg.

For industrial purposes were an increased flow rate is desired, it is important to stay above this value to avoid problems resulting from asphaltene deposition. In Regions II and III shown in the schematic presented in Figure 6, it is possible to mitigate asphaltene deposition by reducing the flow rate. A greater reduction is required in Region II than in III, making a decrease in flow rate most effective for mitigation of deposition under conditions represented by region III.

Another pi group of interest for the deposition of asphaltene in the wellbore is π_{21}. It is a function of the Schmidt number through the definition of N shown in Appendix A. The Schmidt number is a dimensionless ratio of the viscous diffusion rate to the mass diffusion rate of a fluid. An increase in the Schmidt number would decrease the rate of asphaltene deposition in the pipes. As a result, a higher Schmidt number is desired to reduce asphaltene deposition in the wellbore. A relative numerical example, proving this is shown in Appendix D. Since there is only one term in Equation 3.2, various associated fluid properties are analyzed individually or collectively as a

dimensionless group. Other equations involved in describing the deposition process were also scaled to give the pi groups presented in Appendix A for wellbores and pipes.

The dimensionless π_{16} was discovered to have a lot of potential in the definition and classification of asphaltene deposition. Chapter 5 describes the pi group in more detail and utilizes experimental data to validate the speculative relationship with asphaltene deposition shown in this chapter. Further relationships and critical values of pi groups and their effects on asphaltene deposition are also discussed.

Chapter 5: Pi groups – Validation and Discussion

In this chapter, data obtained from previously published experimental results are used to analyze and validate the speculated relationship between the $\boldsymbol{\pi_{16}}$ group and asphaltene deposition. Other relationships are also deduced as a result and another pi group, $\boldsymbol{\pi_{19}}$ is introduced to create a condition for the occurrence of total deposition in the pipes and wellbore.

5.1 Validation of $\boldsymbol{\pi_{16}}$

In this section, the experiments that were conducted and the results that were obtained are shown. Further discussion and relationship between the obtained results and the pi groups obtained are also discussed. It is important to note that the experiments were conducted by the named authors. As a result, the data and results obtained are from previously published works. However, these inferences deduced from the results are utilized to validate the pi group relationships that were discussed in Chapter 4.

5.1.1 Sang J. Park and G. Ali Mansoori, 1988

In this work, the authors attempted to describe the basic mechanisms of organic deposition. They were interested in preventing deposition inside the wellhead and transmission lines by predicting the onset of deposition and the amount of deposition that occur due to various factors. They utilized proposed models to describe the process and then compared the models to experimentally determined results from Hirschberg et al. To determine the solubility properties of the asphaltene, Hirschberg et al carried out titration experiments on tank oil. The onset of precipitation and amount of asphaltene in

the precipitate was then recorded for the crude oil upon dilution with several liquid alkanes. Table 5.1 show the titration results obtained from this work.

Table 5.1 Onset and Amount of Asphaltene Deposition from Tank Oil.

Dilution Ratio (cm^3 diluent/g tank oil)	n-C_5		n-C_7		n-C_{10}	
	EXP[a]	CAL[a]	EXP	CAL	EXP	CAL
1.35						O.F
1.40				O.F	O.F	
1.90	N.T[b]	O.F[c]				
2.22			O.F			
5	—	3.31	1.53	1.52	1.34	1.30
10	3.61	3.67	1.82	2.28	1.45	1.53
20	3.79	3.75	1.89	2.43	1.50	1.45
50	3.87	3.73	1.87	2.29	—	1.13

The experimental titration data (wt% tank oil) are taken from Hirschberg et al. (1983).
[a] EXP = experimental values; CAL = calculated values.
[b] N.T denotes that onset of asphaltene deposition is not determined.
[c] O.F denotes the onset of flocculation.

Sang J. Park and G. Ali Mansoori, used this experimental results and their model to determine the amount of asphaltene deposited from the tank oil when six different paraffin solvents are utilized (Park and Mansoori, 1988). Figure 5.1 shows the results obtained and the match between their model and experimental data.

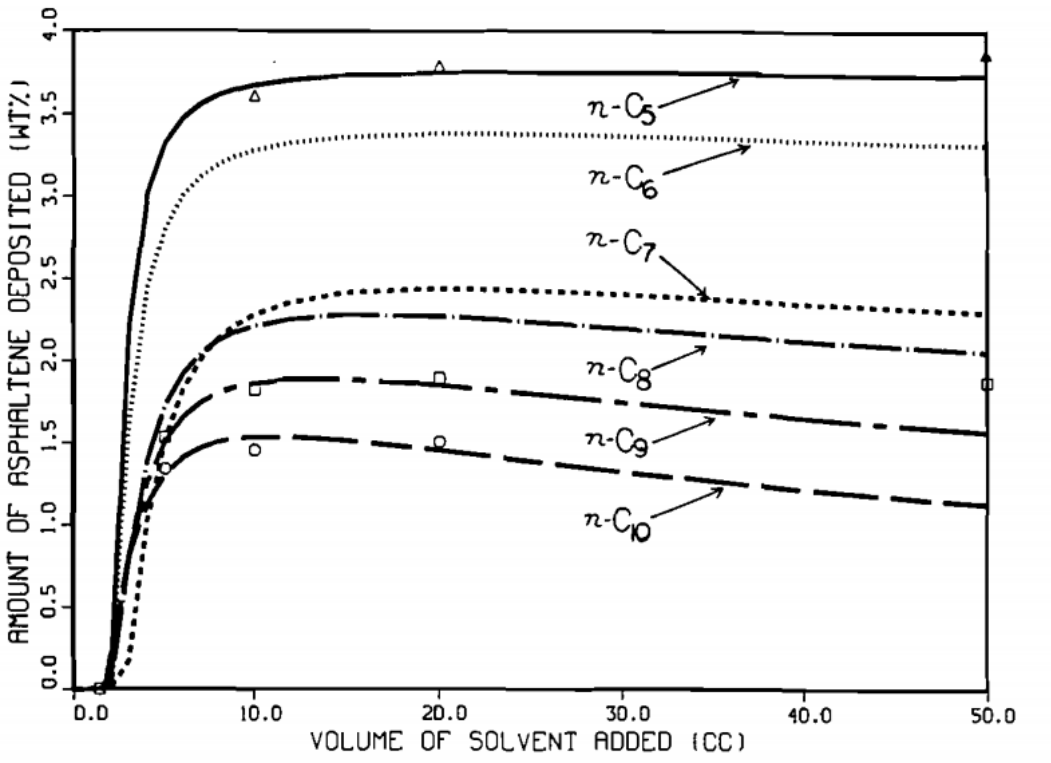

Figure 5.1. Amount of asphaltene deposition from tank oil versus the volume of the paraffin solvents utilized. The experimental deposition data are shown by the dots, while the lines represent the predicted model (Park and Mansoori, 1988).

Based on the experimental results shown in the figure above, $\boldsymbol{\pi_{16}}$ **was** determined for the deposition present in pentane, octane and decane (paraffin with experimental data) using calculated mixture densities of the tank oil and individual alkanes and the concentration of the asphaltene ppt in each mixture shown in Table 5.2. Figure 5.2 shows the relationship between the pi group and amount of asphaltene deposited based on the information provided.

Table 5.2 Calculated variables utilized to determine the deposition relationship with π_{16} based on a 10cc dilution in Figure 5.1.

Alkanes (C-N)	Pentane (C-5)	Octane (C-8)	Decane (C-10)
Calculated mixture densities (g/cm3)	4.79	5.82	6.20
Concentration of asphaltene ppt (g/cm3)	3.61	1.82	1.45
group calculated $\pi_{16}\left[\frac{L}{tu_0}\right]$	1.32	3.20	4.28

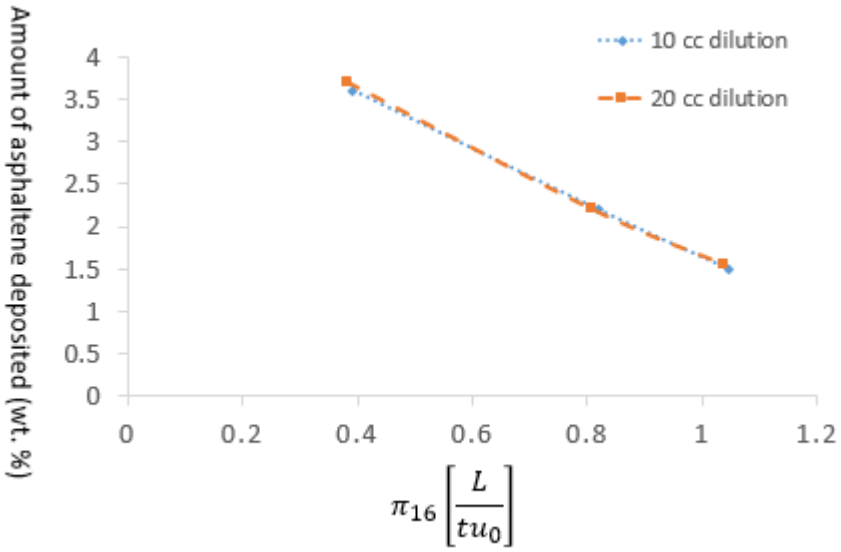

Figure 5.2. Relationship between the $\pi_{16} = \frac{t\rho_0 u_0}{Lc_a}$ group and amount of asphaltene deposition. Where the length of pipe, travel time and the flow velocity are kept constant

The relationship shown in Figure 5.2 verifies that which was expected in Chapter 4 and graphically represented in Figure 4.2. An increase in the pi group would cause a decrease in the total amount of asphaltene deposition occurring in the pipe. For this

experiment, data was not provided for the length of the flow area, so it was assumed constant for all experiments. We also see that the deposition occurring did not change much with an increase in solvent concentration from 10 cc to 20 cc. This can be explained by Figure 5.1 by Hirschberg et al, as further increase in volume from 10 cc had an insignificant effect on the amount of asphaltene deposited.

5.1.2 Peyman Zanganeh et al, 2012

In this work, a novel experimental setup was employed to create a visual cell with high pressure to investigate asphaltene deposition on a model rock. The evolution of the deposition was monitored under a microscope under different conditions. Crudes from two different Iranian oil fields were used and the results obtained were compared visually. Results obtained from these experiments provided a better idea on the different contributing factors to asphaltene deposition. It also gave insights as to what factors had an insignificant effect on the deposition of asphaltene on the model rock.

The experimental setup can be seen in the referenced paper. CO_2 was injected into the setup at varied amounts and comparison of the results showed that an increasing the amount of CO_2 injected increased the amount of asphaltene precipitate deposited. These results are shown in Figure 5.3. The dark particles on in the images are the aggregated asphaltene deposit on the model rock substrate. The amount of injected CO_2 was varied in 5% increments between 5-20 mol % CO_2. Experiments were conducted at 90^0C and 100 bar on the crude gotten from the Kuh-e-mond sample (Zanganeh et al, 2012).

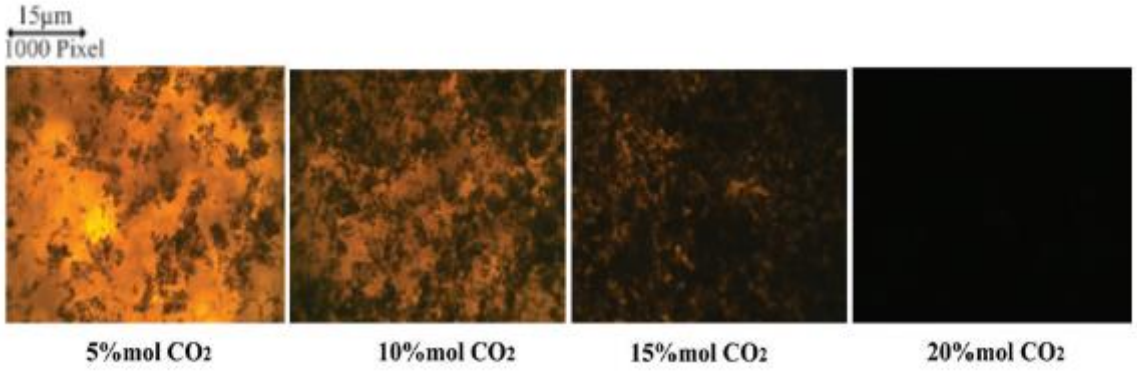

Figure 5.3 Effect of CO2 injection on asphaltene deposition (Zanganeh et al, 2012)

From this figure, one can deduce that an increase in the amount of CO_2 injected into the crude caused an increase in the amount of asphaltene deposited. Zanganeh et al, calculated the amount of asphaltene deposited based on the surface area covered and realized this to be true. From the figure we see that at 20% mol of CO_2 concentration of the injected gas, approximately 100% of the total surface had been covered in asphaltene deposit.

This is relevant to our work done because of the relationship between gas concentration and oil density. An increase in the concentration of the CO_2 in the oil, as with gas injection, decreases the density of the oil. Based on Figure 5.3, a decrease in the density of the oil causes an increase in the amount of asphaltene deposit shown. This goes further to validate the relationship between asphaltene deposition and the pi group. Using density as a reference, a decrease in the density decreases the pi group and increases asphaltene deposition. Therefore, decreasing the pi group would increase asphaltene deposition as expected. Other interesting findings from this work are presented as Figures 5.4 and 5.5 for the Kuh-e-mond and Gachsaran field asphaltene respectively.

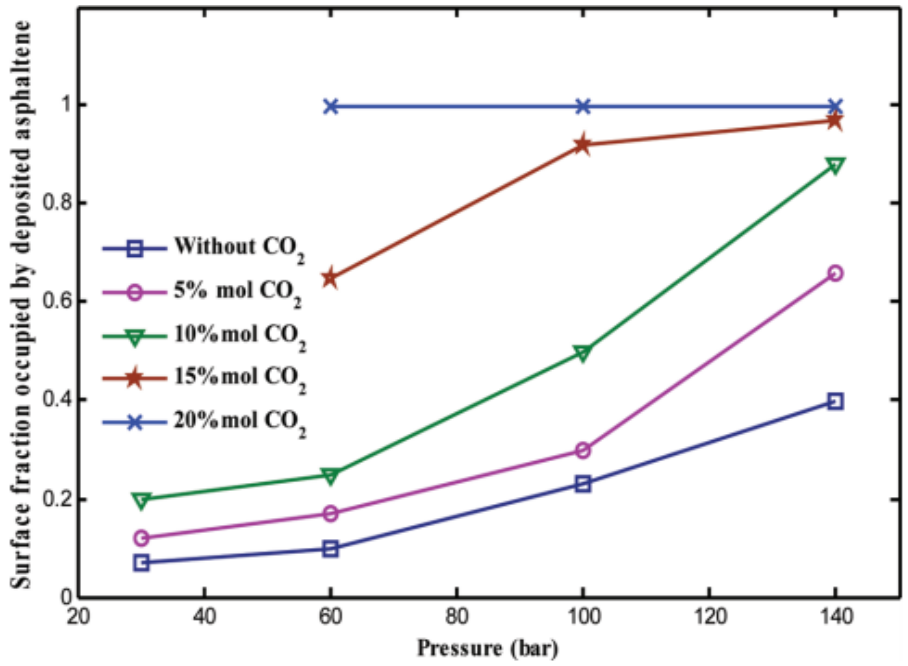

Figure 5.4 Fraction of asphaltene deposit at various pressures for kuh-e-mond asphaltene at different CO_2 concentrations

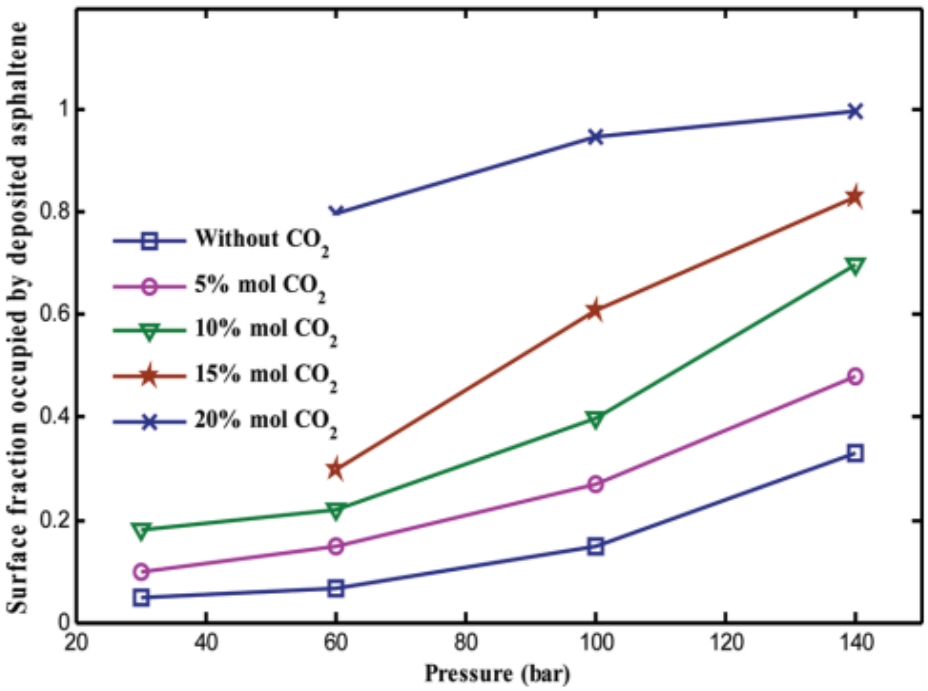

Figure 5.5 Fraction of asphaltene deposit at various pressures for gachsaran asphaltene at different CO_2 concentrations

From both figures we see that a decrease in the density reduces the chances of asphaltene deposition. Using the deposition without CO_2 as a reference in both asphaltene types, we see that an increase in the amount of CO_2 clearly reduces the surface fraction of the substrate occupied by asphaltene and by inference reduces the amount of asphaltene deposited in the substrate. It was also observed in both figures that an increase in the pressure increases the amount of asphaltene deposits even when the concentration of the CO_2 gas injected is kept constant. Although pressure is not a factor defining our pi group, this is an interesting finding and can be explained with relationships based on $\boldsymbol{\pi_{16}}$.

Recalling the definition of $\boldsymbol{\pi_{16}}$, that is $\pi_{16} = \frac{t\rho_0 u_0}{xc_a}$, we see that the pi group would decrease with an increase in ca, which is the concentration of precipitated asphaltene. As a result, we can say that an increase in the ca, would cause an increase in the amount of asphaltene deposited. This is intuitive, as an increase in the abundance of a substance to be deposited should naturally cause an increase in the deposition. However, Figure 5.6 shows the relationship between pressure and the concentration of precipitated asphaltene based on experimental work conducted by Soulgani et al. based on the experimental data obtained, ca decreases with increased pressures. This decreases $\boldsymbol{\pi_{16}}$, and as a result increases the amount of asphaltene deposited, validating Figures 5.4 and 5.5.

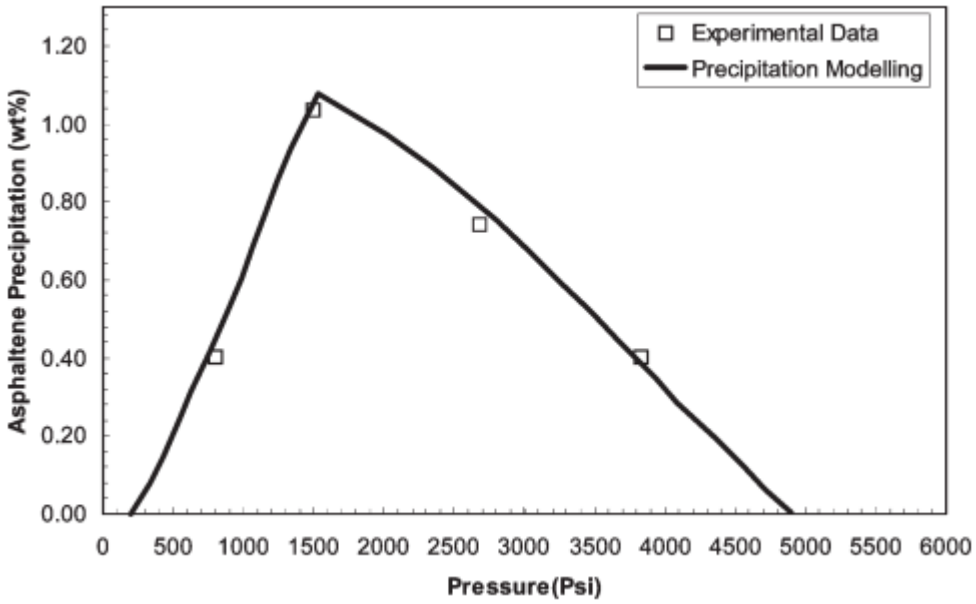

Figure 5.6 Asphaltene precipitate concentration as a function of pressure (Soulgani et al., 2010).

5.2 Further interpretation of π_{16} and its relationship with other pi groups

Based on work experimental work done by Soulgani et al, we were able to further interpret the relationship between the pi group and asphaltene deposition, as well as make modifications to the relationship proposed from the work done.

5.2.1 Interpretation of π_{16} based on experiment by Soulgani et al.

Soulgani et al attempted to model formation damage due to asphaltene deposition and to achieve this, some experiments were conducted. The experimental apparatus utilized determined the mass of the asphaltnee deposited as a function of time by measuring the changes in the thermal resistance resulting from deposition (Soulgani et al, 2010). The heat transfer coefficient was calculated over time since temperature was known and the thermal resistance was then determined This resistance was then converted to mass of

asphaltene deposit using equation 5.1 below. A comprehensive description of the experimental procedures and apparatus utilized is detailed in the work done by Soulgani et al.

$$m_{da} = \rho_d \lambda_d R_A \tag{5.1}$$

Where m_{da} is the mass of asphaltene deposit, ρ_d is the density of the deposit, λ_d is the thermal conductivity of the deposit and R_A is the thermal resistance of the asphaltene deposit calculated based on the heat transfer coefficient and temperatures measured.

Based on the results obtained from the experimental work, models were proposed to describe the relationship between various factors present during production and the rate at which asphaltene deposition occurs. Figure 5.7 shows the plot originated for the relationship between fluid velocity and the rate of asphaltene deposition.

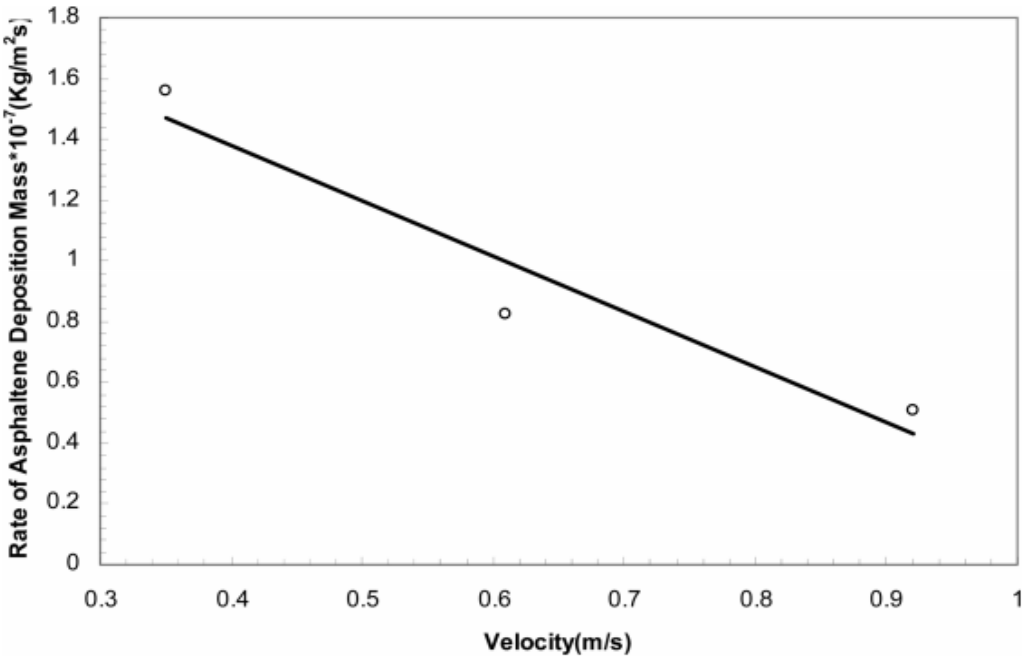

Figure 5.7 Rate of asphaltene deposition as a function of velocity (Soulgani et al., 2010). The line represents the model while the data points are experimental findings.

Soulgani et al. suggested that a linear relationship exists between the velocity and rate of asphaltene deposition, however we found that the relationship is not linear. Our proposed relationship, which we prove in latter parts of this work can be seen in Figure 5.8. Based on the relationship shown in the figure, although an increase in velocity reduces the rate of asphaltene deposition, there exists a critical velocity above which a further increase in the velocity has insignificant effects on the rate of asphaltene deposition. This is important to note for practical purposes to ensure that a cost effective measures are taken to reduce asphaltene deposition optimally.

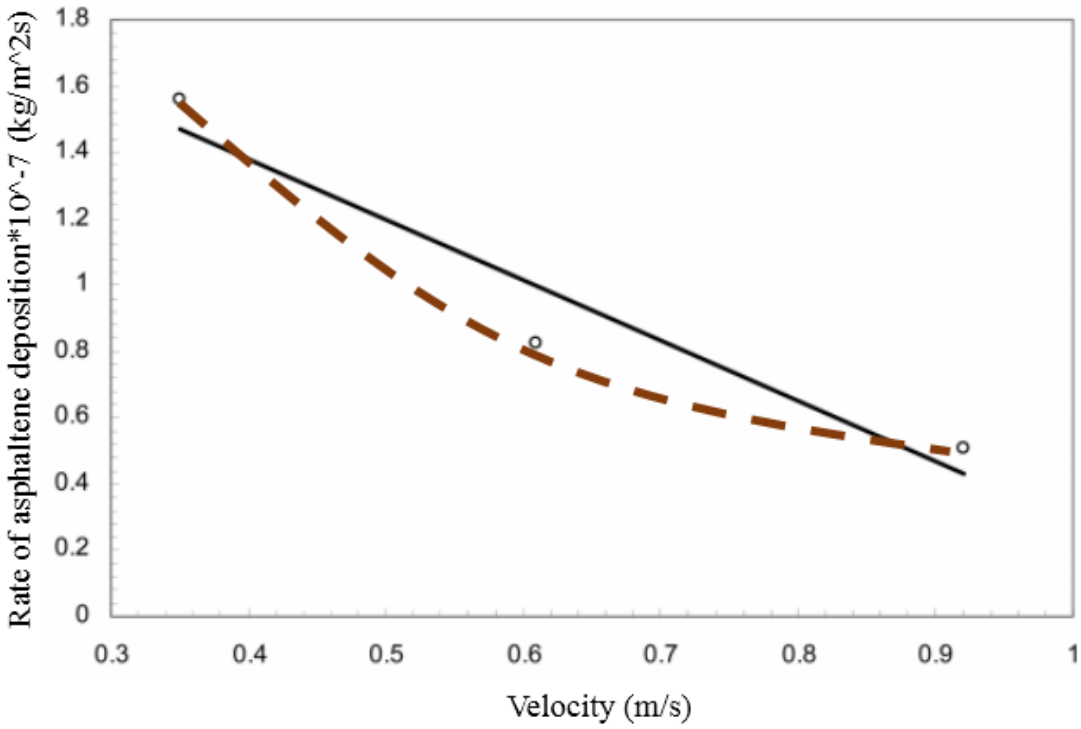

Figure 5.8 Rate of asphaltene deposition as a function of velocity. An increase in the velocity reduces the rate of asphaltene deposition but not linearly. Proposed relationship is shown in dashed line. Original graph by Soulgani et al, 2010.

Using the data obtained from Figure 5.7, π_{16} was calculated at different velocities and plotted for different times. Since the pi group is dependent on time, the calculation was performed for times equaling 200 hours, 400 and 600 hours respectively. Results obtained were plotted and is shown in Figure 5.9 below. From the gra at higher fluid velocities we see that there is a larger $\boldsymbol{\pi_{16}}$ value associated. This is expected, however more interestingly, we can see also that time has a larger effect in the pi group at higher velocities.

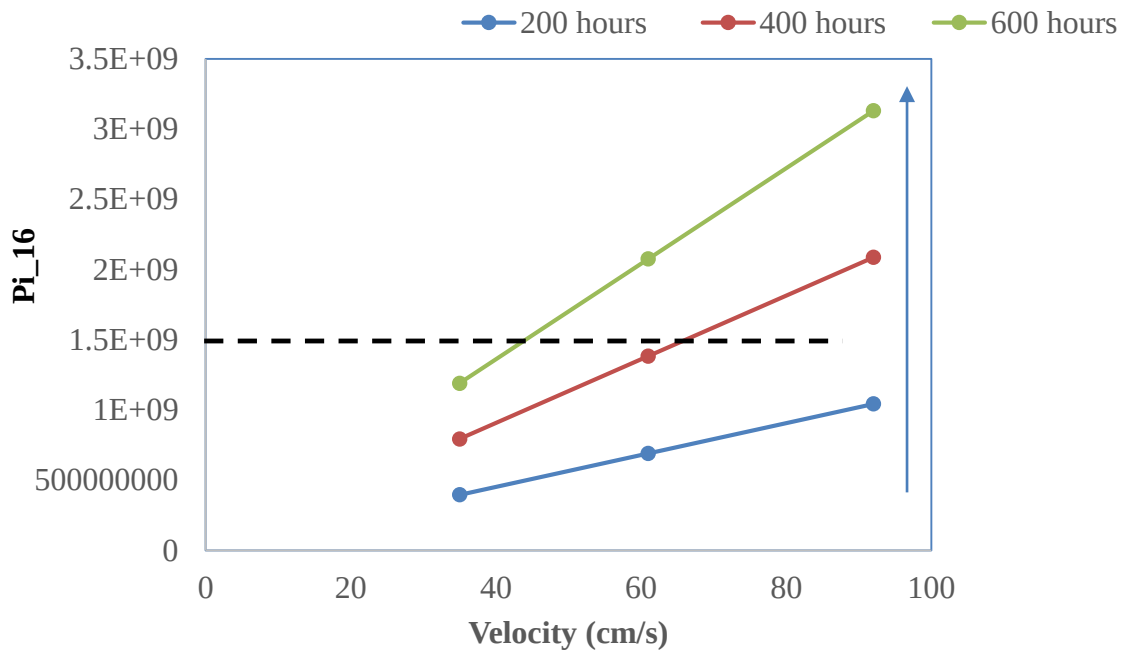

Figure 5.9 Effects of Velocity and Time on $\boldsymbol{\pi_{16}}$ and Asphaltene deposition rate.

The rate at which asphaltene deposition occurs is reduced at higher velocities. This supports the proposed velocity deposition model presented as Figure 5.8. At a decreased velocity, more time is required to get a certain pi group associated with a certain rate of

asphaltene deposition. Time increases upwards as shown by the blue arrow. That is to say, when the velocity is at 60 cm/s only 400 hours is required to get the pi group of 1.5E+09, however 600 hours is required to obtain that same pi group at a velocity of 40 cm/s. It is also important to note that the flow velocity of the fluid scales linearly with the pi group. Therefore $\boldsymbol{\pi_{16}}$ can be used to describe flow behavior at varying velocities during asphaltene deposition.

Figure 5.10 show a graph created with the experimental data of the direct relationship between the velocity and amount of deposit in the pipes. As expected, at higher velocities there is less asphaltene deposit realized in the pipe. We expect this to be the case because of the relationship previously proposed for the pi group and asphaltene deposition in Figure 4.2 and the effects of velocity on the pi group shown in Figure 5.9 above. The calculated pi group was then plotted against the realized deposition rate and the relationship given, shown in Figure 5.11 is similar to that proposed in Chapter 4 with a R^2 value of over 98%, further verifying the assumption.

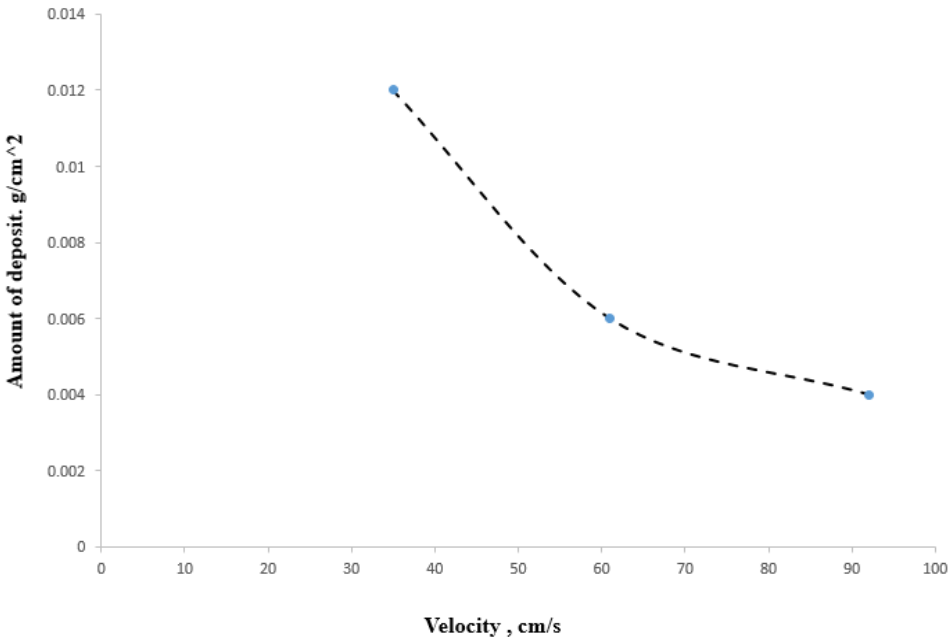

Figure 5.10 Effects of Velocity on Amount of Asphaltene deposit realized in pipe. Experiment by Soulgani et al.

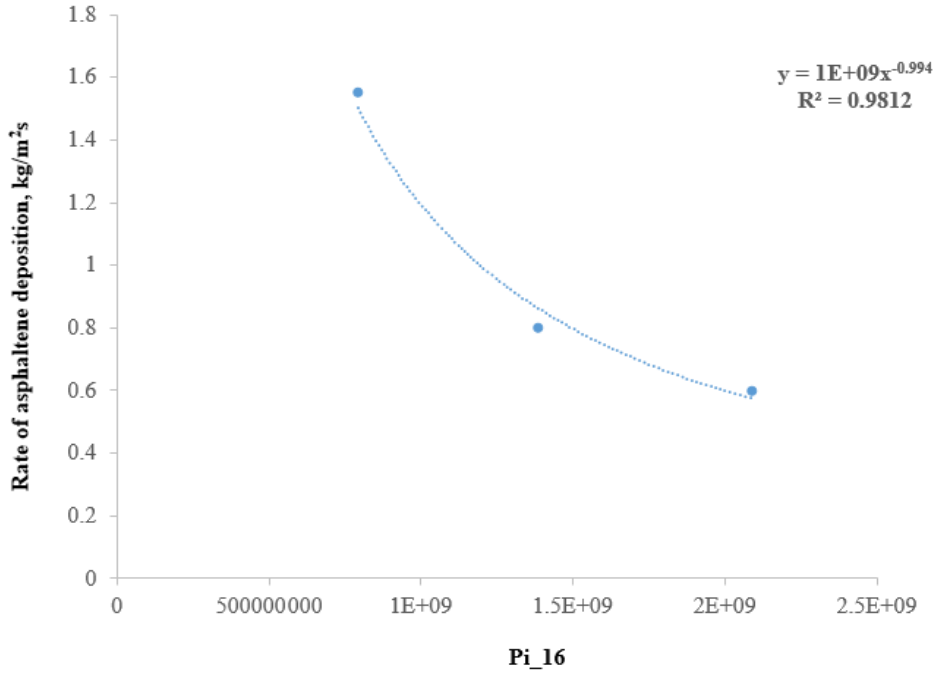

Figure 5.11 Effects of π_{16} on Rate of Asphaltene deposition verified. Experiment by Soulgani et al.

5.2.2 Relationships between pi groups

Other pi groups of interest for the deposition of asphaltene in the wellbore include $\pi_{19}\, and\, \pi_{21}$. $\pi_{21}$is a function of the Schmidt number through the definition of N shown in Appendix A. The Schmidt number is a dimensionless ratio of the viscous diffusion rate to the mass diffusion rate of a fluid. An increase in the Schmidt number would decrease the rate of asphaltene deposition in the pipes. As a result, a higher Schmidt number is desired to reduce asphaltene deposition in the wellbore. A relative numerical example, proving this is shown in Appendix D. Since there is only one term in Equation 2, various associated fluid properties are analyzed individually or collectively as a dimensionless group. Other equations involved in describing the deposition process were also scaled to give the pi groups presented in Appendix A for wellbores and pipes.

Experimental data from Soulgani et al and Hashmi et al were used to calculate the pi groups π_{16} and π_{19}. These groups were plotted against the rate of asphaltene deposition and fitted by the sum of squares linear regression to obtain a mathematical equation defining the existing relationship. Figures 5.12 and 5.13 show the graphs along with the mathematical relationship realized for asphaltene deposition rate as a function of both pi groups. The equation shown in figure 5.12 was plotted for infinite π_{16} values and an ultimate deposition rate was determined. The ultimate deposition rate is defined as the deposition rate to which infinitely large values of the pi group tend towards. All the deposition rates realized from experimental work were then made dimensionless by this ultimate value and plotted against the pi group. With this, the value of π_{16} in which

90% of the total deposition has occurred was determined and named π_{16}^{*}. This is shown in Figure 5.14 and is later utilized to find the equation for the critical velocity proposed in Figure 5.8.

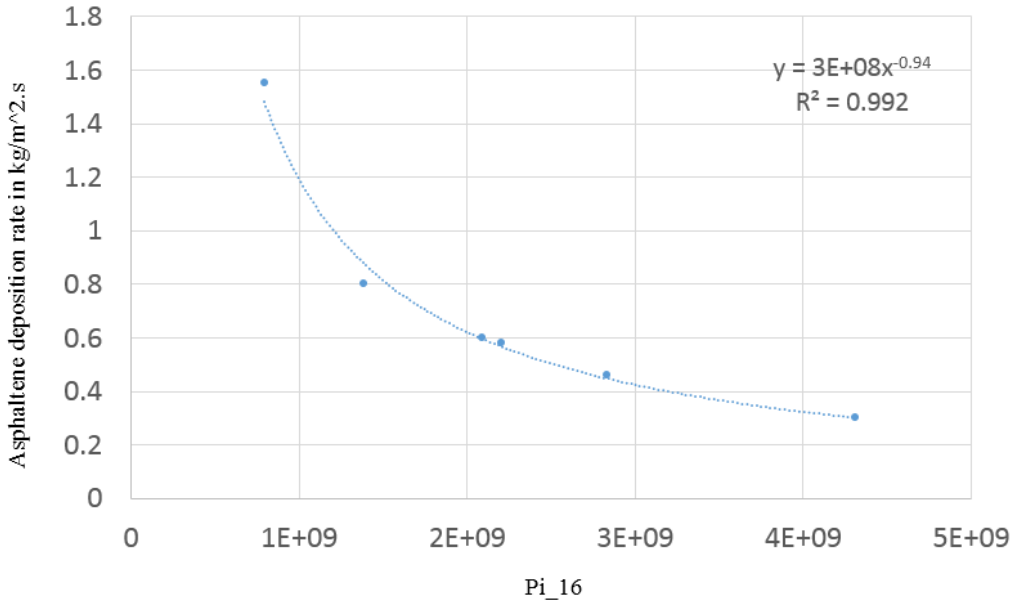

Figure 5.12. Rate of asphaltene deposition as a function of π_{16}. Mathematical equation shown defines the relationship realized.

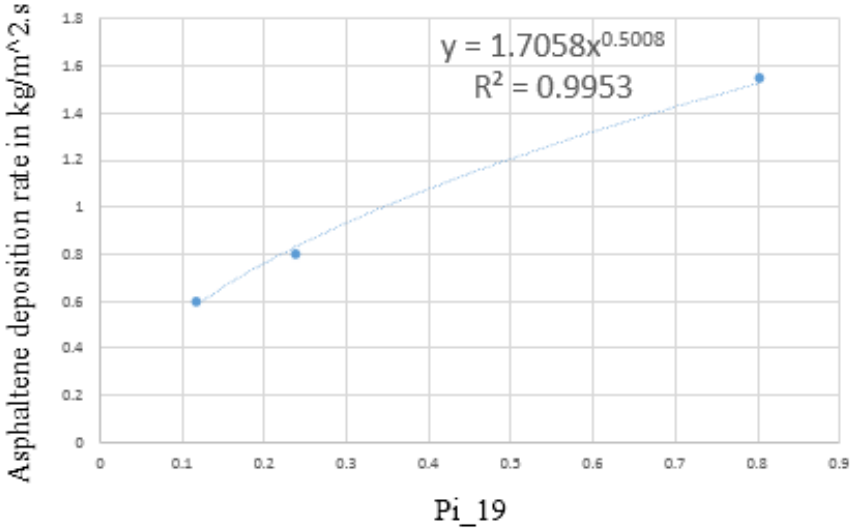

Figure 5.13. Rate of asphaltene deposition as a function of π_{19}. Mathematical equation shown defines the relationship realized.

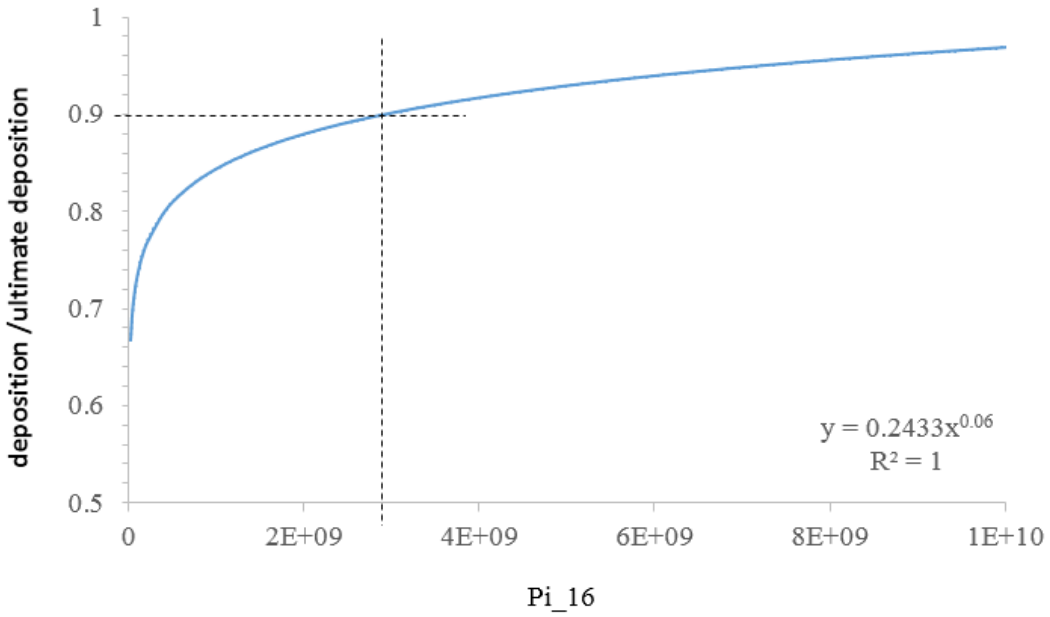

Figure 5.14. Dimensionless asphaltene deposition as a function of π_{16}. π_{16}^{*} is defined as the π_{16} value at which 90% of total deposition has occurred and is approximately equal to 3E + 09

In order to find a relationship between time and the deposition rate, an equality between the two pi groups was initiated based on common terms between the groups, like the length, density and velocity. This relationship is shown in Equation 5.2 and is depicted graphically in Figure 5.15. Based on this relationship and the π_{16}^{*} value at which time 90% of the total possible deposition has occurred, a conditional relationship was formed. This condition is important because it allows the user to determine the time it will take for 90% of the total possible asphaltene deposition to occur. It is shown in Equation 5.3. If the conditional statement is true for any producing well, then 90% of the total deposition has occurred and one can make an informed decision as to whether further deposition would create significant damage where the size of the wellbore is

known. Based on equation 5.3, the critical velocity above which 90% of total deposition has already occurred is given in equation 5.4.

$$mda = [\pi_{16}] * [\pi_{19}] * \frac{ca*\alpha_0}{t} \tag{5.2}$$

$$\frac{3E+09*ca*L}{\rho_0 u_0} \leq t_{90} \tag{5.3}$$

$$V_{critical} = \frac{3E+09*ca*L}{\rho_0 * t_{90}} \tag{5.4}$$

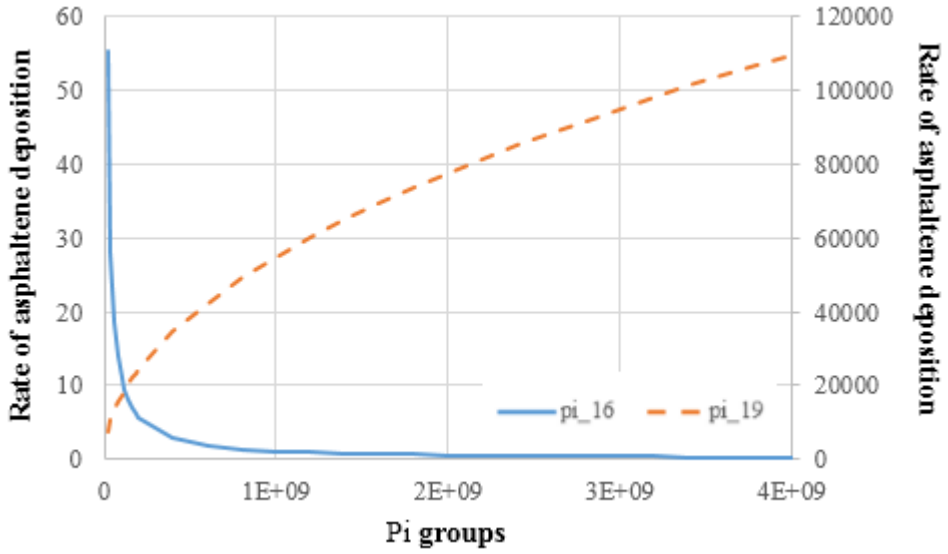

Figure 5.15. Asphaltene deposition as a function both pi groups. The y-scale on the right of the plot is for π_{16} while that on the left is for π_{19}.

The time it will take for 10%, 50% and 90% of total deposition to occur was calculated for different scenarios varying flowrate, length of the pipe and oil density. These graphs and conditions used to calculate this examples are shown in the following section. Results are in line with relationship expected and can serve as an aid for further comprehension of the presented material.

5.3 Upscaling to well scale

The following plots compare the time at which certain levels of deposition take place when the size of the problem area is increased to mimic the flow within the well. The experimental data utilized were collected from various sources and thus they represent different sticking probabilities discussed in section 3.2.2. Therefore, the total deposition, used as the basis for each experiment, varies from one experiment to another; that is, total deposition may either lead to full plugging or not depending on the sticking probability pertinent to the experiment utilized to gain results. Consequently, 10, 50 and 90 % of total deposition does not necessarily signify a full blockage of the pipe.

Generally, an increase in the flow rate causes an increase in fluid velocity at a constant cross sectional area. π_{16} is different for different flowrates and the rate of asphaltene deposition decreases with an increase in π_{16} as shown in Figure 5.12. Based on this, the rate of asphaltene deposition would decrease with an increase in flowrate. This decrease would eventually level off as shown in Figure 5.16. The time it would take to achieve 90% and 50% of total possible deposition is shown at different flowrates in the graph and also in the table within.

Figures 5.17 and 5.18 show the time it would take to achieve 90%, 50% and 10% of total possible deposition with varying oil density and pipe length respectively. An increase in the density reduces the time it would take for the percent deposition of interest to be reached. However, an increase in the length increases the time required. This is the case because an increased length would provide more surface area for

deposition to occur and as a result 90% of deposition for instance in a 8000 ft. pipe would be significantly greater than 90% of the total deposition in a 4000 ft pipe.

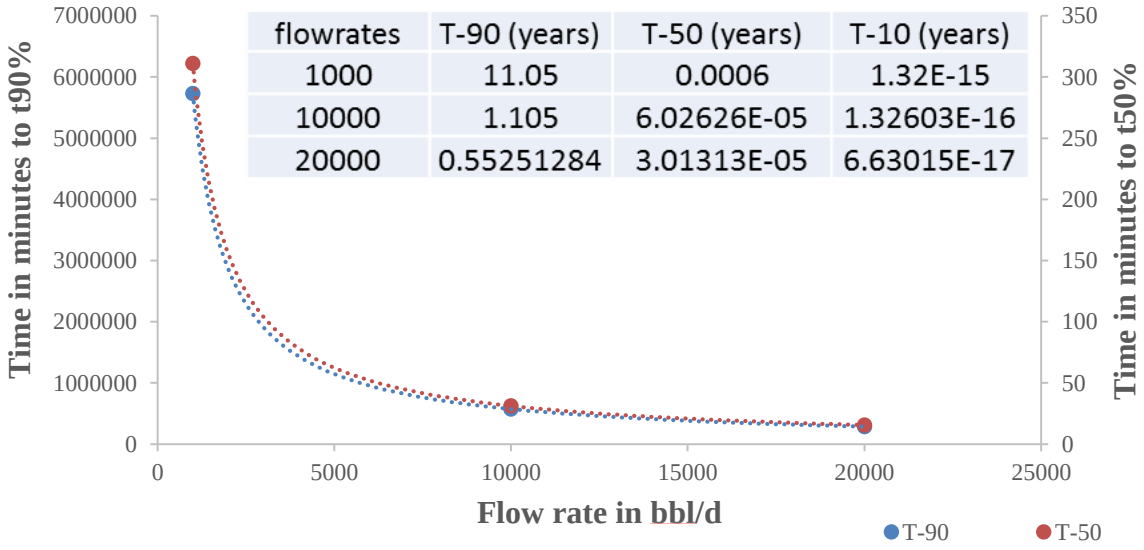

Figure 5.16. The time it takes for 90, 50 and 10% of total asphaltene deposition to occur at varied flowrates in bbl/day. Length was kept constant at 4000 ft, pipe radius at 6.75 inches, density at 800 kg/m^3 and the fraction of asphaltene concentration in oil as 0.04.

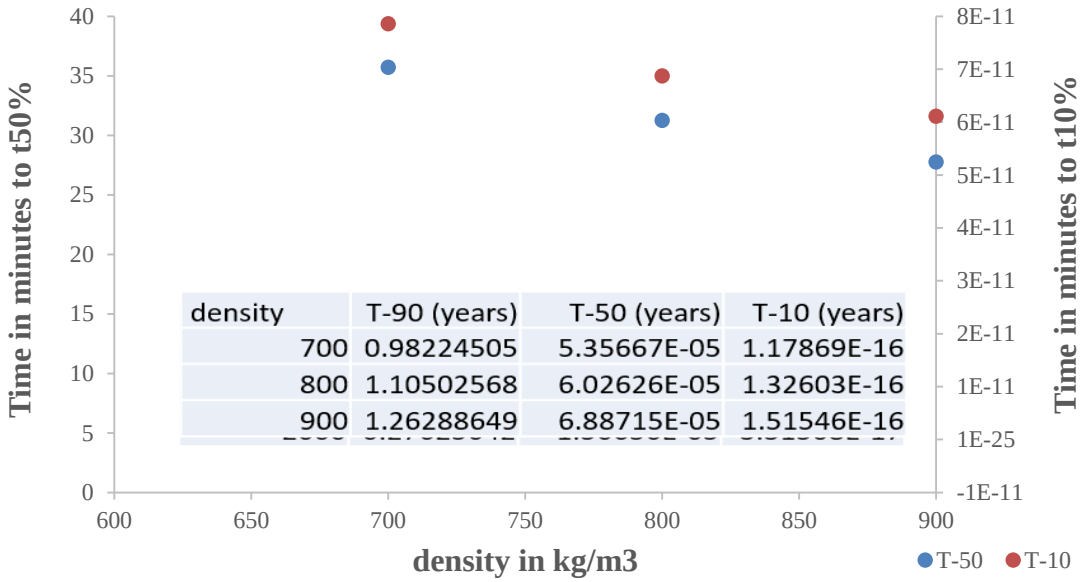

Figure 5.17 The time it takes for 90, 50 and 10% of total asphaltene deposition to occur at varied oil densities in kg/m^3. Length was kept constant at 4000 ft, pipe radius at 6.75 inches, flow rate at 10000 bbl/day and asphaltene concentration in oil at 0.04.

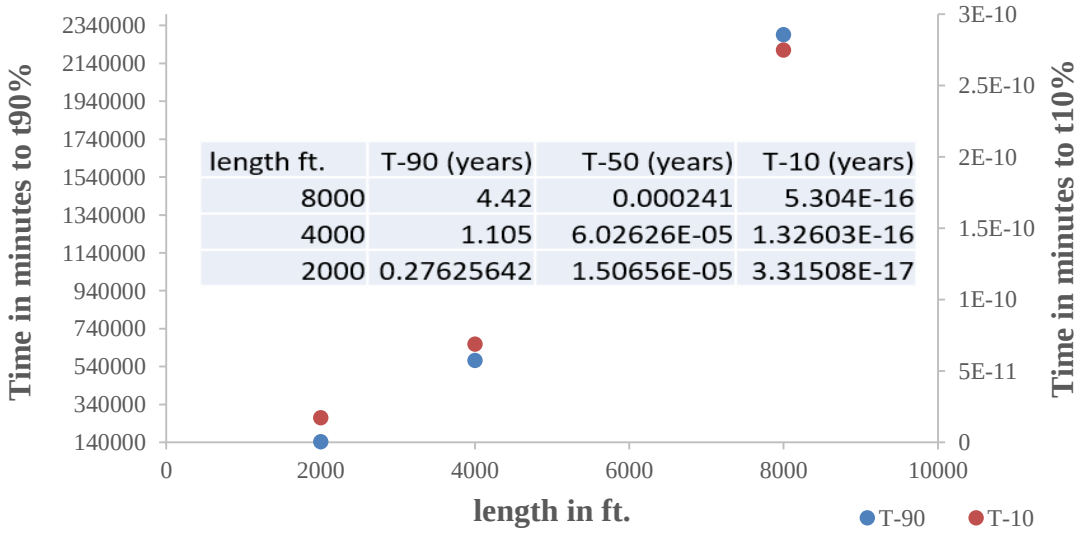

Figure 5.18. Time it takes for 90, 50 and 10% of total asphaltene deposition to occur at varied pipe lengths in ft. Density was kept constant at 800 kg/m^3, pipe

radius at 6.75 inches, flowrate at 10000 bbl/day and asphaltene concentration in oil at 0.04.

Conclusion

Scaling Analysis method is used to simplify and understand the relationship between significant terms in a set of describing equation. In this work asphaltene deposition in porous media and in the pipes are studied with the use of this scaling analysis. Describing equations for both processes are obtained from published literature and are analyzed to form dimensionless pi groups. The pi groups obtained from the deposition in the porous media showed that in specific scenarios, like low porosity formations having insignificant entrainment constant, the driving force of asphaltene deposition would be the surface deposition. This term comprises of the volume fraction of precipitate in the liquid phase and formation porosity. Since formation porosity cannot be changed by the user, it is important that care is taken to reduce the amount of asphaltene deposition in the liquid phase during production.

In the wellbore, scaling analysis was utilized to find a range of critical values of a pi group within which asphaltene deposition can be prevented by decreasing flow rate. They are 51000 cm^3/kg - 16852 cm^3/kg and are obtained from π_{16}. Above the upper bound of this range deposition would not occur for any flow rate utilized and below this range a reduction in the flow rate would not prevent significant asphaltene deposition. Other pi groups were analyzed to interpret the deposition in pipes and experimental data from different authors were used to analyze and validate the relationship amongst the pi groups and also between the pi groups and asphaltene deposition. Based on the understanding gained from the introduction of these pi groups, the assumed relationship between asphaltene deposition and velocity was modified in Chapter 5.

The pi groups analyzed were useful in creating a better description of asphaltene deposition and as a result, a mathematical relationship was determined to define a critical velocity above which an increase in asphaltene deposition would have an insignificant effect on deposition. This critical velocity was determined from the relationship between two pi groups for a certain set of experiments conducted by Soulgani et al and Hashmini et al. Examples of how this critical velocity would affect field applications were also listed in terms of time it would take for a certain percentage of asphaltene deposition to occur under specific field conditions at varied lengths and flowrate. As expected, an increase in the flowrate would decrease the time it would take for certain percentage of deposition to occur and an increase in length would cause an increase in the time it would take for a certain percentage of asphaltene deposition to have occurred in the pipes.

Future Work

In order to further investigate the usefulness of scaling analysis in determining conditions necessary to prevent asphaltene deposition, other dimensionless numbers can be described to better understand ranges above which asphaltene deposition can be inhibited when other properties besides flow rate and velocity are varied. Experiments can be designed and performed based on the relationships obtained from the scaling analysis method to further define the effects of asphaltene deposition in porous media and in pipes. Also software like COMSOL can be utilized for validation purposes. This work introduces the usefulness of scaling analysis and this analysis can be utilized on a wide range of flow assurance problems experienced in the field today.

References

Ali, M. A., and Islam, M. R., "The Effect of Asphaltene Precipitation on Carbonate-Rock Permeability: An Experimental and Numerical Approach", SPE Production & Facilities, August, 1998, 178-183.

Civan, F. and Wang, S. 2005. "Modelling Formation Damage by Asphaltene Deposition during Primary Oil Recovery," ASME, Journal of Energy Resource Technology, Vol 127, December 2005, pp. 310-317.

Civan, F., "Modeling and Simulation of Formation Damage By Organic Deposition", Presented at the First International Symposium in Colloid Chemistry in Oil Production: Asphaltenes and Wax Deposition, ISCOP'95, Rio de Janeiro- RJ-Brazil, November 26-29, 1995, 102-107.

Cleaver, J. W. and Yates, B. 1975. A Sub-layer Model for the Deposition of Particles from a Turbulent Flow. Chem. Eng. Sci, 30, pp983-992, 1975.

Eskin, D., Ratulowski, J., Akbarzadeh, K., and Pan, S.: "Modeling Asphaltene Deposition in Turbulent Pipeline Flows," The Canadian Journal of Chemical Engineering, pp. 421-441, June, 2011.

Gonzalez, D. L., Mahmoodaghdam, E., Lim, F. H., & Joshi, N. B. (2012, January 1). Effects of Gas Additions to Deepwater Gulf of Mexico Reservoir Oil: Experimental Investigation of Asphaltene Precipitation and Deposition. SPE Annual Technical Conference and Exhibition, San Antonio, Texas, 8-10 October. SPE 159098-MS. http://dx.doi.org/10.2118/159098-MS

Hashmini, S. M., Loewenberg, M. and Firoozabadi, A. 2015. "Colloidal asphaltene deposition in laminar pipe flow: Flow rate and parametric effects," Physics of fluid, Vol. 27 AIP Publishing LLC. http://dx.doi.org/10.1063/1.4927221

Hirschberg, A, L. N. J. de Jong, B. A. Schipper, and J. G. Meijers. 1983. Influence of temperature and pressure on asphaltene flocculation. Publication 61, KoninklijkelShell Exploratie en Productie Laboratorium, Rijswijk, The Netherlands.

Hoepfner, M. P., Limsakoune, V., Chuenmeechao, V., Maqbool, T. and Fogler, H. S. (2013). "A Fundamental Study of Asphaltene Deposition," Energy and Fuels, Vol 27, pp. 725-735. American Chemical Society, 2013. dx.doi.org/10.1021/ef3017392

Hutchinson, P.C., Hewitt, G.F., and Dukler, A.E.: "Deposition of Liquid or Solid Dispersions from Turbulent Gas Streams: A Stochastic Model," Chem. Eng. Sci., 26, pp. 419-439, 1971.

Joshi, N.B., Mullins, O.C., Jamaluddin, A., Creek, J. and McFadden, J. "Asphaltene Precipitation from Live Crude Oil," Energy and Fuels, Vol 15, No. 4, 2001, pp. 979-986.

Kohse, B. F. and Nghiem, L. X. 2004. Modelling Asphaltene Precipitation and Deposition in a Compositional Reservoir Simulator. SPE/DOE Symposium on Improved Oil Recovery, Tulsa, Oklahoma, 17-21 April. SPE-89437-MS. http://dx.doi.org/10.2118/89437-MS

Krantz, W. B. 2007. Scaling Analysis in Modelling Transport and Reaction Processes: a systematic approach to model building and the art of approximation. Hoboken, New Jersey: John Wiley & Sons, Inc.

Leontaritis, K. J. 1989. Asphaltene Deposition: A comprehensive Description of Problem Manifestations and Modelling Approaches. SPE Production Operations Symposium, Oklahoma City, Oklahoma, March 13-14. SPE 188892. http://dx.doi.org/10.2118/18892-MS

Leontaritis, K. J., "Asphaltene Near-wellbore Formation Damage Modeling", paper SPE 39446 presented at the SPE Formation Damage Control Conference held in Lafayette, Louisiana, February 18-19, 1998, 277-287.

Lin, C., S., Moulton, R., W., and Putnam, G., L.: "Mass Transfer between Solid and Fluid Streams; Mechanism and Eddy Distribution Relationships in Turbulent Flow," Ind. Eng. Chem, 45, pp. 636-640, 1953.

Mirzayi, B., Mousavi-Dehghani, S. A. and Behruz-Chakan, M. (2013). "Modelling of Asphaltene Deposition in Pipelines," Journal of Petroleum Science and Technology **2013**, 3(2), pp 15-23.

Moghanloo, R. G. 2012. Modelling the Fluid Flow of Carbon Dioxide through Permeable Media. PhD Dissertation, University of Texas at Austin, Austin, Texas (May2012).

Mohammad, T., Mohhammad, N., Rouzbeh, G. M. and Pazuki G.,"Phase Behaviour Assessment of Deposition Compound (Asphaltene) in Heavy Oil," SPE 88753-MS presented at the SPE Abu Dhabi International Conference and Exhibition held in Abu Dhabi, United Arab Emirates, October 10-13, 2004.

Mullins, O. C. (2009). "The Modified Yen Model," Energy and Fuels, Vol 24, 2009, pp. 2179–2207 DOI: 10.1021/ef900975e

Nabzar, L. and Aguilera, M., E. 2008. "A Colloidal Approach. A Promising Route for Asphaltene Deposition Modelling," Oil and Gas Science and Technology-Rev. IFP, Vol. 63, No. 1, pp 21-35. DOI: 10.2516/ogst: 2007083.

Nghiem, L. X., Coombe, D. A., and Ali, F., "Compositional Simulation of Asphaltene Deposition and Plugging", paper SPE 48996 presented at the SPE 73rd Annual Technical Conference and Exhibition held in New Orleans, Louisiana, September 27-30, 1998.

Painter, P., Veytsman, B. and Youtcheff, J. (2015). “Asphaltene Aggregation and Solubility,” Energy and Fuels, Vol 29, 2015, pp. 2120−2133 DOI: 10.1021/ef5024912

Panuganti, S. R., Tavakkoli, M., Vargas, F. M. et al. *In press*. SAFT Model for Upstream Asphaltene Applications. Fluid phase Equilib. (2013).

Pedersen, K. S. and Hasdbjerg C. 2007. PC-SAFT Equation of State Applied to Petroleum Reservoir Fluids. SPE Annual Technical Conference and Exhibition, Anaheim, California, 11-14 November. SPE 110483-MS. http://dx.doi.org/10.2118/110483-MS

Peyman Z, Shahab A,*,† Abdolmohammad A, Ali Z, Hossein D, and Shahin K. “Asphaltene Deposition during CO2 Injection and Pressure Depletion: A Visual Study” Enhanced Oil Recovery (EOR) Research Center, School of Chemical and Petroleum Engineering, Shiraz University, Shiraz, Energy Fuels 2012, 26, 1412−1419 , Irandx.doi.org/10.1021/ef2012744

Ramirez-Jaramillo, E., Lira-Galeana, C. and Manero, O. (2006). “Modeling Asphaltene Deposition in Production Pipelines,” Energy and Fuels, Vol 20, No. 3, 2006, pp. 1184-1196 DOI: 10.1021/ef050262s

Sang J. Park & G. Ali Mansoori (1988) Aggregation and Deposition of Heavy Organics in Petroleum Crudes, Energy Sources, 10:2, 109-125, DOI: 10.1080/00908318808908921

Shirdel, M. 2013. Development of a Coupled Wellbore-Reservoir Compositional Simulator for Damage Prediction and Remediation. PhD dissertation, University of Texas at Austin, Austin, Texas (August 2013).

Soulgani, B., S., Bahman T, Mohammad J and Davood R. 2010. “Modeling Formation Damage due to Asphaltene Deposition in the Porous Media’, Chemical and Petroleum Engineering Department, Sharif University of Technology, November 30, Energy Fuels 2011, 25, 753–761 : DOI:10.1021/ef101195a

Srivastava K. and Huang S. “Asphaltene Deposition During C02 Flooding: A Laboratory Assessment”, Copyright 1997, Society of Petroleum Engineers, Inc. SPE 37468,1997, SPE Production Operations Symposium held in Oklahoma City, Oklahoma, 9-11 March.

Wang S., Civan F. and Strycker A. R., “Simulation of Paraffin and Asphaltene Deposition in Porous Media”, paper SPE 50746 presented at the SPE 1999 International Symposium on Oilfield Chemistry, Houston, Texas. Feb. 16-19, 1999, 57-66.

Wang, J., Buckley, J. Estimate Thickness of Deposit Layer from Displacement Test. 2006. http://baervan.nmt.edu/petrophysics/group/prrc_06-16.pdf (accessed Jan 31, 2013).

Wang, S. 2000. Simulation of Asphaltene Deposition in Petroleum Reservoirs during Primary Oil Recovery. PhD dissertation, University of Oklahoma, Norman, Oklahoma.

Wu, J. and Prausnitz, J. M. 1998. Molecular Thermo-dynamic Framework for Asphaltene-Oil Equilibria. *AICHE* **Vol (44):** 1188-1199. No.5.

Yarranton, H. 2000. Asphaltene Deposition. Canadian International Petroleum Conference, Calgary, Alberta, 4-8 June. PETSOC-2000-099-EA. http://dx.doi.org/10.2118/2000-099-EA

Appendix A: Mathematical equations used to model deposition process

Porous Media

Mass Balance Equations

Oil in liquid phase:

$$\frac{\partial}{\partial t}(\phi \rho_v w_{OL}) + \frac{\partial}{\partial x}(\rho_L u_L w_{OL}) = 0 \quad \text{(A-1)}$$

Asphaltene in liquid phase:

$$\frac{\partial}{\partial t}(\phi C_A \rho_A + \phi \rho_L w_{AL}) + \frac{\partial}{\partial x}(\rho_L u_L w_{SAL} + \rho_L u_L w_{AL}) = -\rho_A \frac{\partial E_A}{\partial t} \quad \text{(A-2)}$$

Asphaltene Deposition Model

$$\frac{\partial E_A}{\partial t} = \propto C_A \phi - \beta E_A (v_L - v_{cr,L}) + \gamma u_L C_A \quad \text{(A-3)}$$

Porosity Reduction Model

$$\phi = \phi_0 - E_A \quad \text{(A-4)}$$

Permeability Reduction Model

$$k = f_p k_0 \left(\frac{\phi}{\phi_0}\right)^3 \quad \text{(A-5)}$$

Momentum Balance Equation

$$u_L = -\frac{k}{\mu_L}\frac{\partial P}{\partial x} \quad \text{(A-6)}$$

Wellbores and Pipes

Mass Balance Equations

Solid Asphaltene in stream:

$$\frac{\partial}{\partial t}(A\rho_o \propto_o + Ac_a \propto_o) + \frac{\partial}{\partial x}(A\rho_o \propto_o u_o + Au_o c_a) = A(\varphi_o + \gamma_a - m_{da}) \tag{A-7}$$

Oil in liquid phase:

$$\frac{\partial}{\partial t}(\rho_o \propto_o) + \frac{1}{A}\frac{\partial}{\partial x}(A\rho_o \propto_o u_o) = \varphi_o \tag{A-8}$$

Cleaver and Yates deposition model definition

$$N = \frac{0.084\Delta C V_{avg}\sqrt{f/2}}{Sc^{2/3}} \tag{A-9}$$

$where\ \Delta C = C_b - C_s$

Rate of Asphaltene attachment

$$m_{da} = \frac{\partial}{\partial x} SP(N) \tag{A-10}$$

Momentum Balance Equation

$$\frac{\partial}{\partial t}(\rho_o u_o) + \frac{\partial}{\partial x}(\rho_o u_o^2) + (144.0 g_c)\frac{\partial P}{\partial x} + \rho_0 g sin\theta + \frac{\tau_o \pi D}{A} = 0 \tag{A-11}$$

Appendix B: Table Showing Pi groups obtained

$Pi\ number$	$Defining\ dimensionless\ group$
π_1	$\frac{t\rho_L u_L}{x\rho_v \phi}$
π_2	$\frac{\rho_L w_{AL}}{C_A \rho_A}$
π_3	$\frac{t\rho_L u_L w_{SAL}}{x\phi C_A \rho_A}$
π_4	$\frac{t\rho_L u_L w_{AL}}{x\phi C_A \rho_A}$
π_5	$\frac{E_A}{\phi C_A}$
π_6	$\frac{1}{\phi}$
π_7	$\frac{E_A}{\phi}$
π_8	$f_p \frac{\phi}{k}$
π_9	$\frac{kp}{\mu_L x u_L}$
π_{10}	$\frac{\alpha C_A \phi}{\beta E_A \Delta v}$
π_{11}	$\frac{1}{t\Delta v \beta}$
π_{12}	$\frac{\gamma C_A u_L}{\beta E_A \Delta v}$
π_{13}	$\frac{L}{x}$

π_{14}	$\frac{c_a}{\rho_0 \alpha_0}$
π_{15}	$\frac{x}{t u_0}$
π_{16}	$\frac{t \rho_0 u_0}{x c_a}$
π_{17}	$\frac{x \varphi_0}{\rho_0 \alpha_0 u_0}$
π_{18}	$\frac{x \gamma_a}{\rho_0 \alpha_0 u_0}$
π_{19}	$\frac{x m_{da}}{\rho_0 \alpha_0 u_0}$
π_{20}	$\frac{t \varphi_0}{\rho_0 \alpha_0}$
π_{21}	$\frac{SpN}{m_{da} x}$

Table 1-Pi groups obtained from scaling analysis of the asphaltene deposition models in porous media near the wellbore and also in pipes.

Appendix C: Data utilized to analyze $\pi_{16} = \frac{t\rho_0 u_0}{x c_a}$ for pipe deposition

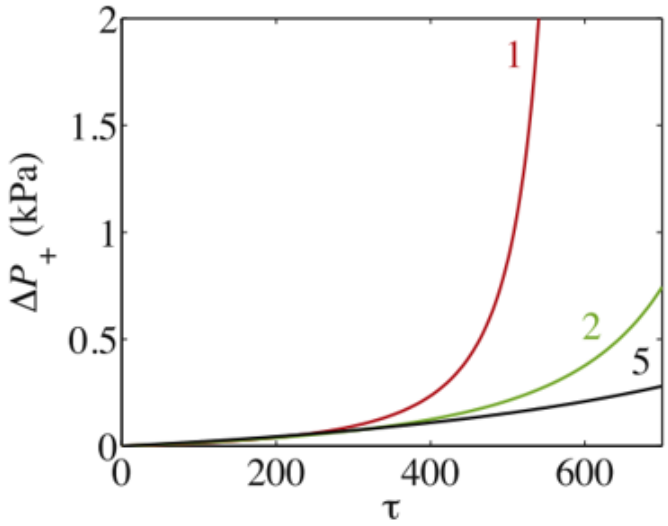

Parameters	
V	0.24 cm³
A	0.0079 cm²
x	30 cm
ca	0.0248 kg/cm³

Figure C-1. Effect of Q- flow rate on the difference in pressure drop in a pipe. Flow rates are written in colors and are in cm^3/hr. Models were made from raw experimental data obtained by Hashmi et al. Aligned parameters, also collected experimentally, are used to calculate the pi group and are calculated as a function of fluid density.

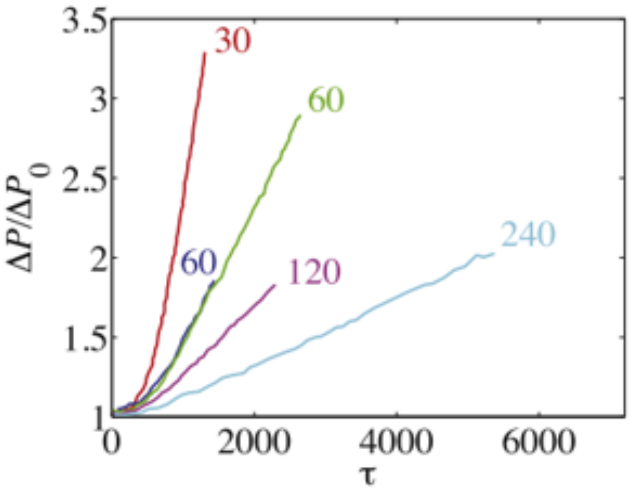

Parameters	
V	0.425 cm³
A	0.0085 cm²
x	50 cm
ca	0.0248 kg/cm³

Figure C-2. Effect of Q- flow rate on the difference in pressure drop in a pipe, shown by raw data by Nabzar and Aguilera. Flow rates are written in colors and are in cm^3/hr. Aligned parameters, also collected experimentally, are used to calculate the pi group

and are calculated as a function of fluid density. In calculating the fluid velocity, $u_0 = \frac{Q_0}{A}$.

Appendix D: Numerical example showing the effects of Schmidt number on Asphaltene deposition using Scaling Analysis

Starting from Equation 2, re-written below:

$$m_{da} = \frac{\partial}{\partial x} SP \left(\frac{0.084 \Delta C V_{avg} \sqrt{f/2}}{Sc^{2/3}} \right)$$

The equation can be rewritten as shown in Equation C-1

$$m_{da} = 0.084 V_{avg} \sqrt{f/2} \frac{\partial}{\partial x} SP \left(\frac{\Delta C}{Sc^{2/3}} \right) \quad \text{D-1}$$

Defining unspecified scale and reference factors yields

$$m^*_{da} m_{da_s} = 0.084 SPV_{avg} \sqrt{f/2} \frac{\partial}{\partial x^* x_s} \left(\frac{\Delta C^* \Delta C_s}{Sc^{*2/3} {Sc_s}^{2/3}} \right) \quad \text{D-2}$$

Forming dimensionless variables and introducing them into describing equations yields

$$m^*_{da} = \left[\frac{0.084 SPV_{avg} \sqrt{f/2} \Delta C_s}{m_{da_s} x_s {Sc_s}^{2/3}} \right] \frac{\partial}{\partial x^*} \left(\frac{\Delta C^*}{Sc^{*2/3}} \right) \quad \text{D-3}$$

C-3 is equal to Equation C-4 by the definition of N in the Nomenclature. Note that the coefficient in C-4 is equal to π_{21}

$$m^*_{da} = \left[\frac{SpN}{m_{da_s} x_s} \right] \frac{\partial}{\partial x^*} \left(\frac{\Delta C^*}{Sc^{*2/3}} \right) \quad \text{D-4}$$

With all other variables remaining unchanged, an increase in the Schmidt number from 1 to 1000 would reduce N by a multiple of 0.001. This would reduce the coefficient in C-4 by an equal manner causing a 1000th place reduction in the rate of solid asphaltene deposition in the pipes, denoted by mda^*.

Appendix E: Original plot of asphaltene deposition rate as a function of velocity proposed by Soulgani et al

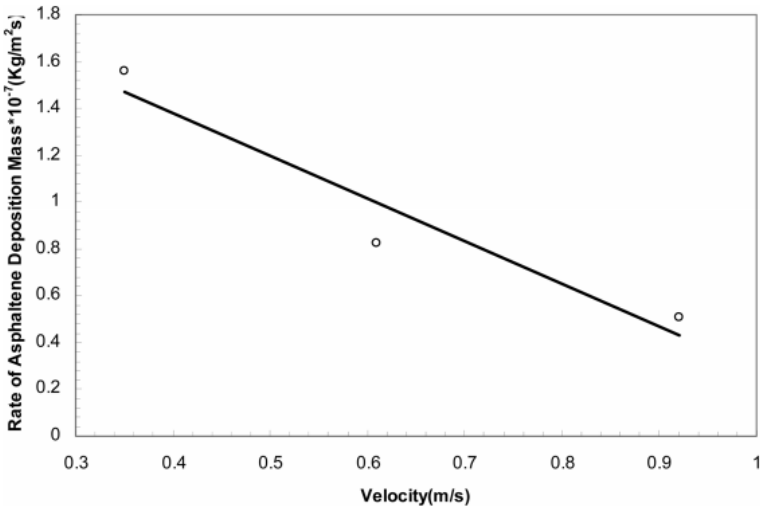

Figure E.1: Velocity vs. rate of asphaltene deposition by Soulgani et al, 2010

Appendix F: Nomenclature

Porous deposition

t = time, (s)

x = distance, (ft)

ϕ = porosity

ρ_v = density of vapor phase, (lb/gal)

w_{OL} =mass fraction of the oil component in the liquid phase

ρ_L = density of liquid phase, (lb/gal)

u_L =fluxes in the liquid phase, (cm/s)

C_A =volume fraction of suspended asphaltene precipitates in the liquid phase

ρ_A =density of asphaltene, (lb/gal)

w_{AL} =mass fraction of the dissolved asphaltene in the liquid phase

w_{SAL} = mass fraction of the suspended asphaltene precipitates in the liquid phase

E_A =volume fraction of the deposited asphaltene in the bulk volume of the porous media

$\propto$= surface deposition rate coefficient, (1/s)

β = entrainment rate coefficient, (1/cm)

$v_L = \frac{u_L}{\phi}$ = intersticial velocity of liquid phase (cm/s)

$v_{cr,L}$ =critical intersticial velocity of liquid phase, a constant, (cm/s)

γ =instantenous plugging deposition rate coefficient, (1/s)

k =absolute permeability of the porous media, (md)

f_p =permeability modification coefficient, constant

p =pressure of fluids in the pore volume, (psia)

μ_L =viscosity of the liquid phase, (cp)

Pipe deposition

A =Pipe cross sectional area (ft^2)

ρ_o =density of oil, (lb/gal)

$\propto_o$=volume fraction of oil

c_a =asphaltene concentration in the crude oil (lbm/ft^3)

u_o =velocity of oil (cm/s)

φ_o =molar flux of oil between the wellbore and reservoir

γ_a =flocculation of solid asphaltene particles

m_{da} =deposition rate of solid asphaltene, ($lbm/s.ft^3$)

K_t = global mass transfer coefficient, (m/sec)

$V_{avg}\sqrt{f/2}$ =Average friction velocity

$Sc = \frac{\mu}{\rho D_B}$ = Schmidt number

N =total mass flux, (lbm/s)

SP = Sticking probability

g_c =acceleration due to gravity – conversation factor

P =pressure, (psi)

g = acceleration due to gravity, (ft/s^2)

τ_o =initial shear stress, ($lbm/s^2.ft$)

D = pipe diameter, (ft)